The Thesis Committee for William Zachary Corse
Certifies that this is the approved version of the following thesis:

Green's Function Methods in 1D Nanoscale Electron Waveguides

APPROVED BY

SUPERVISING COMMITTEE:

Linda E. Reichl, Supervisor

Duane Dicus

Green's Function Methods in 1D Nanoscale Electron Waveguides

by

William Zachary Corse, B.S.

THESIS

Presented to the Faculty of the Graduate School of

The University of Texas at Austin

in Partial Fulfillment

of the Requirements

for the Degree of

MASTER OF ARTS

THE UNIVERSITY OF TEXAS AT AUSTIN

December 2014

Dedicated to my family and friends.

Green's Function Methods in 1D Nanoscale Electron Waveguides

William Zachary Corse, M.A.
The University of Texas at Austin, 2014

Supervisor: Linda E. Reichl

R-matrix theory has been used to analyze a variety of scattering potentials in ballistic electron waveguides. The S-matrix is the principal result of this method. Here we analyze ballistic electron scattering in a 1D waveguide with a step potential at its terminus using Green's function theory. We calculate the S-matrix for this system, scattering particles' quasibound states, and the survival probability of a particle initially localized in the step region. We then apply R-matrix theory to the same problem. In doing so, we demonstrate the versatility of the Green's function approach, but also its relative complexity.

Table of Contents

Abstract **v**

List of Tables **ix**

List of Figures **x**

Chapter 1. Introduction **1**

Chapter 2. Green's Function for a Particle in a 1D Square Well **3**
2.1 Problem Setup 3
2.2 Energy Eigenstates 4
2.3 Green's Function 5
2.4 Poles 7
2.5 Residues 7
2.6 Free Particle 9

Chapter 3. Green's Function for a Particle in a Partitioned 1D Square Well **10**
3.1 Problem Setup 10
3.2 Energy Eigenstates 11
3.3 $\mathbf{G}_Q^o$ 13
3.4 $\mathbf{G}_P^o$ 14
3.5 **QGQ** 15
3.6 **PGP** 19

Chapter 4. Green's Function for a Particle in a 1D Well with a Step Potential **22**
4.1 Problem Setup 22
4.2 Energy Eigenstates 24
4.3 $\mathbf{G}_Q^o$ 24

4.4 $\mathbf{G}_P^o$ . . . 25
4.5 **QGQ** . . . 26
4.6 **PGP** . . . 26

Chapter 5. Poles and Residues of the Green's Functions for the 1D Well and 1D Waveguide 28
5.1 Well Poles . . . 28
5.2 Waveguide Poles . . . 30
5.3 Well Residues . . . 30
5.4 Waveguide Residues . . . 34

Chapter 6. Survival Probabilities of Particles in the Reaction Region of the 1D Waveguide 37
6.1 Gaussian Initial State . . . 37

Chapter 7. Calculating the S-matrix for a 1D Step Potential from the Green's Function 40
7.1 Limiting form of $\mathbf{G}_P^o$ . . . 40
7.2 **PGP** Revisited . . . 41
7.3 Reflection Amplitude . . . 44

Chapter 8. Reaction Function Methods 46
8.1 Reaction Function Definition . . . 46
8.2 Calculating the S-Matrix from the Reaction Function . . . 47
8.3 Re-summing the S-matrix . . . 48
8.4 Poles of the S-matrix . . . 49

Chapter 9. Conclusion 51

Appendix 53
10.1 Summation Formula for 2.17 . . . 54
10.2 Summation Formula for 3.21 . . . 55
10.3 Calculating $\langle x_1|\mathbf{G}_Q^o\mathbf{QHPG}_P^o\mathbf{PHQG}_Q^o|x_2\rangle$ . . . 55
10.4 Re-summing the S-matrix . . . 57

Bibliography **60**

Vita **62**

List of Tables

8.1 Numerical comparisons of Poles 50

List of Figures

2.1 1D Square Well 4

3.1 1D Partitioned Square Well 11

4.1 1D Well with Step Potential 23
4.2 1D Waveguide with Step Potential 23

5.1 Well poles 29
5.2 Waveguide poles 31
5.3 Well residues 31
5.4 $L \to 0$ well residues 33
5.5 First waveguide quasibound state probability distribution 34
5.6 Second waveguide quasibound state probability distribution 35

6.1 Gaussian initial particle state 38
6.2 Survival probability for a Gaussian initial particle state 39

Chapter 1

Introduction

In the late 1940s, Wigner and Eisenbud developed reaction matrix scattering theory to explain observed nuclear scattering data [1]. In R-matrix theory, the scatterer is confined to a finite reaction region that is singularly coupled to asymptotic space [2, 3]. Given a set of fixed boundary conditions, wave functions are expanded in terms of a complete set of basis states in the reaction region and are then coupled to free particle states in the adjacent asymptotic space. Procedurally, in R-matrix theory, one calculates the reaction matrix for a scattering process, from which the S-matrix follows.

In addition to nuclear scattering theory, R-matrix theory has been used to analyze numerous other scattering applications, most notably ballistic electron waveguides [4–8]. A ballistic electron waveguide is typically formed at a GaAs/Al_xGa_{1-x}As interface [9–11]. A two-dimensional gas is located ∼500 Å below the surface of the GaAs/Al_xGa_{1-x}As heterostructure. Leads (asymptotic scattering regions) and cavities (reaction regions) of any shape are formed by attaching metal gates to the heterostructure and applying a negative voltage. At sufficiently low temperatures (T∼0.1-2.0 K) electron waves travel ballistically through these cavities and leads, since electron-phonon scattering interactions have a comparatively small mean free path and phase decoherence due to electron-electron scattering is negligible [12].

One can also use the Green's function solution to Schrödinger's equation to study scattering processes [13]. Like the reaction matrix in R-matrix theory, the Green's function (expressed in energy coordinates) can be constructed from a complete set of energy basis states. Furthermore, the Green's function for a scattering system can be partitioned across multiple regions in coordinate space, such as asymptotic and reaction regions. Like in R-matrix theory, these regions must be singularly coupled. The Green's function for a scattering system contains more information than the S-matrix however. From it, one can calculate a particle's propagator, energy poles, quasibound states, survival probabilities, and the S-matrix itself.

In the following sections, we will apply Green's function theory to study 1D nanoscale ballistic electron waveguides. Note that we confine our analyses to 1D for demonstration purposes, but the results that follow are easily generalizable to two dimensions. We begin with calculating the Green's function for a particle in a 1D square well in section two. Section three partitions the square well into two regions. In section four, we add a step potential and extend the closed well into an open system by an analytic continuation of the Green's function. In section five, we calculate the poles and residues of the Green's functions for these open and closed systems. In section six, we calculate the survival probability of a particle placed in the reaction region of the open step potential. In section seven, we derive the S-matrix for this model. Finally, in section eight, we revisit the same model but use R-matrix theory to demonstrate its relative simplicity as well as its limitations.

Chapter 2

Green's Function for a Particle in a 1D Square Well

We begin with the classic 1D square well. The theory and machinery laid down here will serve as a foundation for more nuanced problems later in the paper. We first identify the energy eigenstates for the 1D square well and then construct the Green's function that is unique to this system from these eigenstates. We then show that the poles of the Green's function for this particular closed system are the energy eigenvalues associated with the eigenstates from which we originally calculated the Green's function. The residues of the Green's function will be shown to be related to the eigenstates of the system. Finally, we demonstrate that taking the limit of the Green's function for the square well as one wall goes to infinity produces the Green's function for a free particle incident on a hard wall.

2.1 Problem Setup

The 1D square well is described by the potential (see figure 2.1)

$$V(x) = \begin{cases} \infty & x \leq 0 \\ 0 & 0 < x < L + a \\ \infty & x \geq L + a \end{cases} \tag{2.1}$$

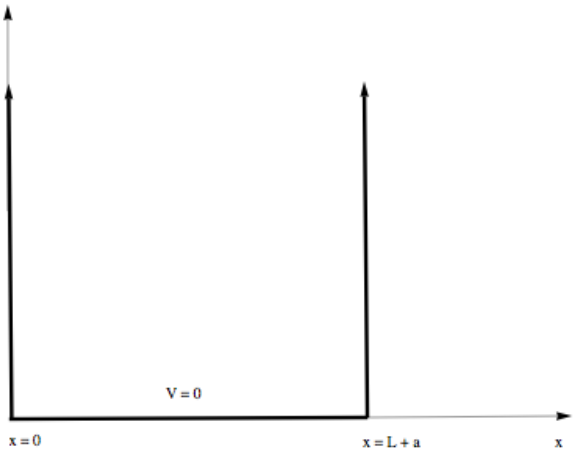

Figure 2.1: 1D Square Well

2.2 Energy Eigenstates

The energy eigenstates of a particle in this potential must satisfy the time-independent Schrödinger equation,

$$\mathbf{H}\Psi_n(x) = -\frac{\hbar^2}{2m}\frac{\partial^2}{\partial x^2}\Psi_n(x) = E_n\Psi_n(x) \tag{2.2}$$

subject to the boundary conditions

$$\Psi_n(0) = 0 \tag{2.3}$$

$$\Psi_n(L+a) = 0 \tag{2.4}$$

Solving, we find that

$$\Psi_n(x) = \langle x|E_n\rangle = \sqrt{\frac{2}{L+a}}\sin\left(\frac{n\pi x}{L+a}\right) \tag{2.5}$$

with

$$E_n = \frac{\hbar^2 n^2 \pi^2}{2m\left(L+a\right)^2} \tag{2.6}$$

These eigenstates are both complete:

$$\sum_{n=1}^{\infty}\langle x_1|E_n\rangle\langle E_n|x_2\rangle = \delta\left(x_1 - x_2\right) \tag{2.7}$$

and orthonormal:

$$\langle E_n|E_{n'}\rangle = \int_0^{L+a} dx\langle E_n|x\rangle\langle x|E_{n'}\rangle = \delta_{n,n'} \tag{2.8}$$

With a discrete, complete, and orthonormal set of basis states in hand, we can now construct the Green's function for this system.

2.3 Green's Function

The general Green's function for Schrödinger's equation satisfies

$$i\hbar\frac{\partial \mathbf{G}\left(t;t_0\right)}{\partial t} - \mathbf{H}\mathbf{G}\left(t;t_0\right) = \delta\left(t-t_0\right) \tag{2.9}$$

The solution to this equation is given by

$$\mathbf{G}\left(t;t_0\right)=e^{-\frac{i}{\hbar}\mathbf{H}(t-t_0)}\Theta\left(t-t_0\right) \tag{2.10}$$

For $t>t_0=0$ and $z=E+i\delta$, we can use the Laplace transform of this solution to express $\mathbf{G}\left(t\right)$ in terms of complex energy coordinates, z:

$$\mathbf{G}\left(z\right)=\int_o^\infty dte^{\frac{i}{\hbar}zt}\mathbf{G}\left(t\right) \tag{2.11}$$

$$=\frac{\mathbf{I}}{z\mathbf{I}-\mathbf{H}} \tag{2.12}$$

We proceed to calculate the spatial matrix elements of $\mathbf{G}\left(z\right)$ for $x_1>x_2$ as follows:

$$\langle x_1|\mathbf{G}\left(z\right)|x_2\rangle=\sum_{n,n'}\langle x_1|E_n\rangle\langle E_n|\mathbf{G}\left(z\right)|E_{n'}\rangle\langle E_{n'}|x_2\rangle \tag{2.13}$$

$$=\left(\frac{2}{L+a}\right)\sum_{n=1}^{\infty}\frac{\sin\left(\frac{n\pi x_1}{L+a}\right)\sin\left(\frac{n\pi x_2}{L+a}\right)}{z-\frac{\hbar^2\pi^2n^2}{2m(L+a)^2}} \tag{2.14}$$

$$=\left(\frac{-2m}{(L+a)\hbar^2}\right)\sum_{n=1}^{\infty}\frac{\cos\left[\frac{n\pi(x_1-x_2)}{L+a}\right]-\cos\left[\frac{n\pi(x_1+x_2)}{L+a}\right]}{\frac{n^2\pi^2}{(L+a)^2}-\frac{2mz}{\hbar^2}} \tag{2.15}$$

$$=\frac{1}{2}\sqrt{\frac{2m}{z\hbar^2}}\frac{\cos\left[(L+a+x_2-x_1)\sqrt{\frac{2mz}{\hbar^2}}\right]-\cos\left[(L+a-x_1-x_2)\sqrt{\frac{2mz}{\hbar^2}}\right]}{\sin\left[(L+a)\sqrt{\frac{2mz}{\hbar^2}}\right]} \tag{2.16}$$

$$=-\sqrt{\frac{2m}{z\hbar^2}}\frac{\sin\left[(L+a-x_1)\sqrt{\frac{2mz}{\hbar^2}}\right]\sin\left[x_2\sqrt{\frac{2mz}{\hbar^2}}\right]}{\sin\left[(L+a)\sqrt{\frac{2mz}{\hbar^2}}\right]} \tag{2.17}$$

(see 10.1 for details of the summation formula applied in this derivation). If $x_2 > x_1$, then

$$\langle x_1|\mathbf{G}(z)|x_2\rangle = -\sqrt{\frac{2m}{z\hbar^2}}\frac{\sin\left[(L+a-x_2)\sqrt{\frac{2mz}{\hbar^2}}\right]\sin\left[x_1\sqrt{\frac{2mz}{\hbar^2}}\right]}{\sin\left[(L+a)\sqrt{\frac{2mz}{\hbar^2}}\right]} \tag{2.18}$$

2.4 Poles

We can now extract the same information that went into preparing the Green's function by looking at its poles and residues in the complex energy plane. While this may not seem immediately useful, when we later extend a closed system to an open one, we will see that this same process allows us to calculate quasibound states and survival probabilities.

The poles of 2.17 are the values of z for which its denominator is zero, which is true when $z = \dfrac{\hbar^2 n^2 \pi^2}{2m(L+a)^2}$. These are the eigenvalues of the system.

2.5 Residues

The residues of the Green's function for this system give us the eigenfunctions in the square well. If we select the contour to enclose a single pole, then we extract the eigenfunction associated with that pole:

$$-\Psi_n(x_1)\Psi_n^*(x_2) = \frac{1}{2\pi i}\int_C \langle x_1|G(z)|x_2\rangle dz \tag{2.19}$$

$$= \lim_{z\to E_n}(z-E_n)\langle x_1|G(z)|x_2\rangle \tag{2.20}$$

which we solve as follows:

$$\lim_{z\to E_n}\sqrt{\frac{2m}{z\hbar^2}}\frac{z-\frac{\hbar^2n^2\pi^2}{2m(L+a)^2}}{\sin\left[(L+a)\sqrt{\frac{2mz}{\hbar^2}}\right]}=\frac{2m\left(L+a\right)}{\hbar n\pi}\frac{1}{\cos\left[(L+a)\sqrt{\frac{2mz}{\hbar^2}}\right]\Big|_{z=E_n}} \tag{2.21}$$

$$=(-1)^n\frac{2}{L+a} \tag{2.22}$$

Note the use of L'Hôspital's rule. Meanwhile,

$$\sin\left[x_2\sqrt{\frac{2mz}{\hbar^2}}\right]\Big|_{z=E_n}=\sin\left[\frac{n\pi x_2}{L+a}\right] \tag{2.23}$$

and

$$\sin\left[(L+a-x_1)\sqrt{\frac{2mz}{\hbar^2}}\right]\Big|_{z=E_n}=\sin\left[n\pi-\frac{n\pi x_1}{L+a}\right] \tag{2.24}$$

$$=(-1)^{n+1}\sin\left[\frac{n\pi x}{L+a}\right] \tag{2.25}$$

Combining these expressions, we see that

$$\Psi_n\left(x_1\right)\Psi_n^*\left(x_2\right)=\frac{2}{L+a}\sin\left[\frac{n\pi x_1}{L+a}\right]\sin\left[\frac{n\pi x_2}{L+a}\right] \tag{2.26}$$

If $x_2=x_1$, then the square root of the above expression yields the eigenfunctions of this system: $\Psi_n\left(x_1\right)=\sqrt{\frac{2}{L+a}}\sin\left[\frac{n\pi x_1}{L+a}\right]$.

2.6 Free Particle

In the limit that L is large (expanding the right wall of the well to infinity), we can write

$$\lim_{L\to\infty} \langle x_1|\mathbf{G}\left(z\right)|x_2\rangle = i\sqrt{\frac{m}{2z\hbar^2}}\left[e^{i(x_1+x_2)\sqrt{\frac{2mz}{\hbar^2}}} - e^{i(x_1-x_2)\sqrt{\frac{2mz}{\hbar^2}}}\right] \tag{2.27}$$

which is the Green's function for a particle incident on a hard wall.

Chapter 3

Green's Function for a Particle in a Partitioned 1D Square Well

We now examine the same potential, but partition the well into two regions, Q and P. While this complicates the mathematics of an otherwise simple problem, it facilities the substitution of arbitrary potentials into a localized region for study. The goals of this section are the same as those of the previous one, but require some extra steps to reach. As will be shown, without a potential in the well, the two partitions of the Green's function, as well as the unpartitioned Green's function for the entire well, are all identical.

3.1 Problem Setup

This time, we describe the well potential as follows (see figure 3.1):

$$V(x) = \begin{cases} \infty & x < 0 \\ 0 & 0 \leq x < a \\ 0 & a \leq x \leq L + a \\ \infty & x > L + a \end{cases} \tag{3.1}$$

and define the regions Q and P such that

$$Q = \{x : x \in [0, a]\} \tag{3.2}$$

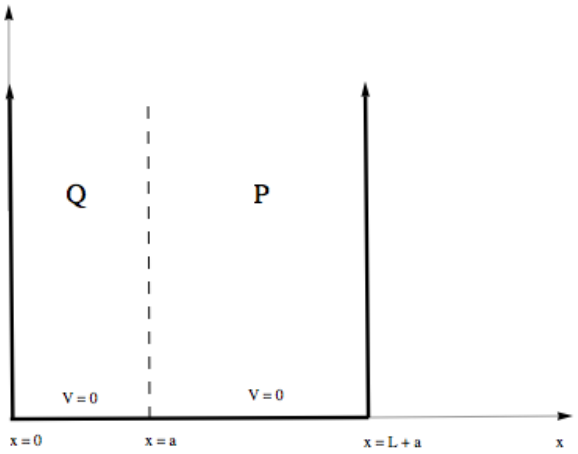

Figure 3.1: 1D Partitioned Square Well

$$P = \{x : x \in [a, L + a]\} \tag{3.3}$$

Meanwhile, $\mathbf{Q}$ and $\mathbf{P}$ will represent the projection operators for their respective regions. Since the potential is infinite outside the well, for all intents and purposes, $\mathbf{Q}+\mathbf{P} = \mathbf{I}$. Furthermore, $\mathbf{Q}^2 = \mathbf{Q}$ and $\mathbf{P}^2 = \mathbf{P}$. For future purposes, we consider Q to be the reaction region.

3.2 Energy Eigenstates

The eigenfunctions in regions P and Q must both satisfy the time-independent Schrödinger equation:

$$-\frac{\hbar^2}{2m}\frac{d^2}{dx^2}\Psi_n = E\Psi_n \tag{3.4}$$

Because the particle is inside an infinite well, it must be the case that

$$\Psi_n^Q(0) = 0 \tag{3.5}$$

$$\Psi_n^P(L+a) = 0 \tag{3.6}$$

The Wigner-Eisenbud method requires that the eigenfunctions in the reaction region obey a zero-slope boundary condition at the interface between the reaction region and the rest of the system (located in this problem at $x = a$). There is some flexibility in the choice of boundary condition at $x = a$ in region P, but in this case, we force the eigenfunctions in P to be zero at $x = a$ in order to mimic the well problem in the previous section. These boundary conditions can be written

$$\frac{d\Psi_n^Q}{dx}(a) = 0 \tag{3.7}$$

$$\Psi_n^P(a) = 0 \tag{3.8}$$

$$\tag{3.9}$$

The following eigenfunctions and eigenvalues satisfy these conditions in Q:

$$\Psi_n^Q = \sqrt{\frac{2}{a}} \sin\left[\frac{(2n-1)\pi x}{2a}\right] \tag{3.10}$$

$$E_n^Q = \frac{\hbar^2 \pi^2 (2n-1)^2}{8ma^2} \tag{3.11}$$

$$n = 1, 2, 3, \ldots \tag{3.12}$$

and in P:

$$\Psi_n^P = \sqrt{\frac{2}{L}} \sin\left[\frac{n\pi\left(x-a\right)}{L}\right] \tag{3.13}$$

$$E_n^P = \frac{\hbar^2\pi^2 n^2}{2mL^2} \tag{3.14}$$

$$n = 1, 2, 3, \ldots \tag{3.15}$$

3.3 $\mathbf{G}_Q^o$

We now calculate the spatial matrix elements of $\mathbf{G}_Q^o$, which will be used later when we calculate the projections of the Green's function, $\mathbf{QGQ}$ and $\mathbf{PQP}$. $\mathbf{G}_Q^o$ is defined by

$$\mathbf{G}_Q^o = \frac{\mathbf{Q}}{z\mathbf{Q} - \mathbf{QHQ}} \tag{3.16}$$

This calculation proceeds in the same manner as the one for $\langle x_1|\mathbf{G}\left(z\right)|x_2\rangle$ in the previous section, but relies on a different summation formula. If $x_1 > x_2$, then

$$\langle x_1|\mathbf{G}_Q^o\left(z\right)|x_2\rangle = \sum_{n=1}^{\infty} \frac{\langle x_1|\Psi_n^Q\rangle\langle\Psi_n^Q|x_2\rangle}{z - \frac{\hbar^2\pi^2(2n-1)^2}{8ma^2}} \tag{3.17}$$

$$= -\frac{16m}{a\hbar^2} \sum_{n=1}^{\infty} \frac{\sin\left[\frac{(2n-1)\pi x_1}{2a}\right] \sin\left[\frac{(2n-1)\pi x_2}{2a}\right]}{\frac{(2n-1)^2\pi^2}{a^2} - \frac{8mz}{\hbar^2}} \tag{3.18}$$

$$= -\frac{8m}{a\hbar^2} \sum_{n=1}^{\infty} \frac{\cos\left[\frac{(2n-1)\pi}{2a}\left(x_1 - x_2\right)\right] - \cos\left[\frac{(2n-1)\pi}{2a}\left(x_1 + x_2\right)\right]}{\frac{(2n-1)^2\pi^2}{a^2} - \frac{8mz}{\hbar^2}} \tag{3.19}$$

$$= -\frac{1}{2}\sqrt{\frac{2m}{z\hbar^2}}\frac{\sin\left[(a-x_1+x_2)\sqrt{\frac{2mz}{\hbar^2}}\right]-\sin\left[(a-x_1-x_2)\sqrt{\frac{2mz}{\hbar^2}}\right]}{\cos\left[a\sqrt{\frac{2mz}{\hbar^2}}\right]} \tag{3.20}$$

$$= -\sqrt{\frac{2m}{z\hbar^2}}\frac{\cos\left[(a-x_1)\sqrt{\frac{2mz}{\hbar^2}}\right]\sin\left[x_2\sqrt{\frac{2mz}{\hbar^2}}\right]}{\cos\left[a\sqrt{\frac{2mz}{\hbar^2}}\right]} \tag{3.21}$$

(see 10.2 for details of the summation formula applied in this derivation). If $x_2 > x_1$, then

$$\langle x_1|\mathbf{G}_Q^o(z)|x_2\rangle = -\sqrt{\frac{2m}{z\hbar^2}}\frac{\cos\left[(a-x_2)\sqrt{\frac{2mz}{\hbar^2}}\right]\sin\left[x_1\sqrt{\frac{2mz}{\hbar^2}}\right]}{\cos\left[a\sqrt{\frac{2mz}{\hbar^2}}\right]} \tag{3.22}$$

3.4 $\mathbf{G}_P^o$

This calculation closely resembles the one for $\mathbf{G}_Q^o$. We define $\mathbf{G}_P^o$ by

$$\mathbf{G}_P^o = \frac{\mathbf{P}}{z\mathbf{P}-\mathbf{PHP}} \tag{3.23}$$

If $x_1 > x_2$, then

$$\langle x_1|\mathbf{G}_P^o(z)|x_2\rangle = \sum_{n=1}^{\infty}\frac{\langle x_1|\Psi_n^P\rangle\langle\Psi_n^P|x_2\rangle}{z-\frac{\hbar^2\pi^2n^2}{2mL^2}} \tag{3.24}$$

$$= -\frac{4m}{L\hbar^2}\sum_{n=1}^{\infty}\frac{\sin\left[\frac{n\pi(x_1-a)}{L}\right]\sin\left[\frac{n\pi(x_2-a)}{L}\right]}{\frac{n^2\pi^2}{L^2}-\frac{2mz}{\hbar^2}} \tag{3.25}$$

$$= -\sqrt{\frac{2m}{z\hbar^2}}\frac{\sin\left[(L+a-x_1)\sqrt{\frac{2mz}{\hbar^2}}\right]\sin\left[(x_2-a)\sqrt{\frac{2mz}{\hbar^2}}\right]}{\sin\left[L\sqrt{\frac{2mz}{\hbar^2}}\right]} \tag{3.26}$$

If $x_2 > x_1$, then

$$\langle x_1|\mathbf{G}_P^o(z)|x_2\rangle = -\sqrt{\frac{2m}{z\hbar^2}}\frac{\sin\left[(L+a-x_2)\sqrt{\frac{2mz}{\hbar^2}}\right]\sin\left[(x_1-a)\sqrt{\frac{2mz}{\hbar^2}}\right]}{\sin\left[L\sqrt{\frac{2mz}{\hbar^2}}\right]} \tag{3.27}$$

3.5 QGQ

We are now in a position to calculate the projection of the Green's function, $\mathbf{G}(z)$, in the region Q, thereby obtaining **QGQ**. We begin the Green's function solution to Schrödinger's equation:

$$(z\mathbf{I}-\mathbf{H})\mathbf{G}(z) = \mathbf{I} \tag{3.28}$$

and operate with operator $\mathbf{Q}$ to the left and right of both sides of the expression to get

$$z\mathbf{QGQ} - \mathbf{QHGQ} = \mathbf{Q}^2 = \mathbf{Q} \tag{3.29}$$

Next we insert the identity between $\mathbf{H}$ and $\mathbf{G}$, and recalling that $\mathbf{Q}^2 = \mathbf{Q}$ and $\mathbf{P}^2 = \mathbf{P}$, we write

$$z\mathbf{QGQ} - \mathbf{QHQQGQ} - \mathbf{QHPPGQ} = \mathbf{Q} \tag{3.30}$$

thus

$$\mathbf{QGQ} = \frac{\mathbf{Q}}{z\mathbf{Q} - \mathbf{QHQ}} + \frac{\mathbf{QHPPGQ}}{z\mathbf{Q} - \mathbf{QHQ}} \tag{3.31}$$

$$= \mathbf{G}_Q^o + \mathbf{G}_Q^o\mathbf{QHPPGQ} \tag{3.32}$$

Returning to 3.28, but this time operating on the left with $\mathbf{P}$ and on the right with $\mathbf{Q}$, we find that

$$\mathbf{PGQ} = \mathbf{G}_P^o\mathbf{PHQQGQ} \tag{3.33}$$

If we insert 3.33 into 3.32, we get that

$$\mathbf{QGQ} = \mathbf{Q}\left[z\mathbf{Q} - \mathbf{QHQ} - \mathbf{QHPG}_P^o\mathbf{PHQ}\right]^{-1}\mathbf{Q} \tag{3.34}$$

We can expand $\mathbf{QGQ}$ as follows:

$$\mathbf{QGQ} = \mathbf{Q}\left[z\mathbf{Q} - \mathbf{QHQ} - \mathbf{QHPG}_P^o\mathbf{PHQ}\right]^{-1} \tag{3.35}$$

$$= \mathbf{Q}\left[z\mathbf{Q} - \mathbf{QHQ}\right]^{-1}\left[1 - \left[z\mathbf{Q} - \mathbf{QHQ}\right]^{-1}\mathbf{QQHPG}_P^o\mathbf{PHQ}\right]^{-1} \tag{3.36}$$

$$= \left[1 - \mathbf{G}_Q^o\mathbf{QHPG}_P^o\mathbf{PHQ}\right]^{-1}\mathbf{G}_Q^o \tag{3.37}$$

$$= \left(1 + \mathbf{G}_Q^o\mathbf{QHPG}_P^o\mathbf{PHQ} + \mathbf{G}_Q^o\mathbf{QHPG}_P^o\mathbf{PHQG}_Q^o\mathbf{QHPG}_P^o\mathbf{PHQ} + \ldots\right)\mathbf{G}_Q^o \tag{3.38}$$

Hence,

$$\langle x_1|\mathbf{QGQ}|x_2\rangle = \langle x_1|\mathbf{G}_Q^o|x_2\rangle + \langle x_1|\mathbf{G}_Q^o\mathbf{QHPG}_P^o\mathbf{PHQG}_Q^o|x_2\rangle + \\ \langle x_1|\mathbf{G}_Q^o\mathbf{QHPG}_P^o\mathbf{PHQ}\left(\mathbf{G}_Q^o\mathbf{QHPG}_P^o\mathbf{PHQ}\right)^1\mathbf{G}_Q^o|x_2\rangle + \ldots + \\ \langle x_1\mathbf{G}_Q^o\mathbf{QHPG}_P^o\mathbf{PHQ}\left(\mathbf{G}_Q^o\mathbf{QHPG}_P^o\mathbf{PHQ}\right)^n\mathbf{G}_Q^o|x_2\rangle + \ldots \tag{3.39}$$

We have already calculated $\langle x_1|\mathbf{G}_Q^o|x_2\rangle$, and would now like to focus on the second term in the expansion. To calculate $\langle x_1|\mathbf{G}_Q^o\mathbf{QHPG}_P^o\mathbf{PHQG}_Q^o|x_2\rangle$, we insert the identity twice, but restrict the limits of integration to the region covered by the operator $\mathbf{Q}$:

$$\langle x_1|\mathbf{G}_Q^o\mathbf{QHPG}_P^o\mathbf{PHQG}_Q^o|x_2\rangle = \int_0^a\int_0^a dx_3dx_4\langle x_1|\mathbf{G}_Q^o|x_3\rangle\langle x_3|\mathbf{QHPG}_P^o\mathbf{PHQ}|x_4\rangle\langle x_4|\mathbf{G}_Q^o|x_2\rangle \tag{3.40}$$

The inner bracket, $\langle x_3|\mathbf{QHPG}_P^o\mathbf{PHQ}|x_4\rangle$, can also be expanded, but this time the operator $\mathbf{P}$ restricts the limits of integration to the region P:

$$\langle x_3|\mathbf{QHPG}_P^o\mathbf{PHQ}|x_4\rangle = \int_a^{L+a}\int_a^{L+a} dx_5dx_6\langle x_3|\mathbf{QHP}|x_5\rangle\langle x_5|\mathbf{G}_P^o|x_6\rangle\langle x_6|\mathbf{PHQ}|x_4\rangle \tag{3.41}$$

Note the coupling terms $\mathbf{QHP}$ and $\mathbf{PHQ}$ that link regions P and Q. These are defined to be [14]

$$\mathbf{QHP} = -\frac{2\hbar^2}{m}\mathbf{Q}\boldsymbol{\partial}_x^{\rightarrow}\delta\left(x-a\right)\mathbf{P} \tag{3.42}$$

$$\mathbf{PHQ} = -\frac{2\hbar^2}{m}\mathbf{P}\boldsymbol{\partial}_x^{\leftarrow}\delta\left(x-a\right)\mathbf{Q} \tag{3.43}$$

where the arrows on the partial derivatives indicate the directions in which they should act. The details of these calculations are outlined in 10.3. We find that

$$\langle x_3|\mathbf{QHPG}_P^o\mathbf{PHQ}|x_4\rangle = \frac{2\hbar^2}{m}\sqrt{\frac{2mz}{\hbar^2}}\cot\left[L\sqrt{\frac{2mz}{\hbar^2}}\right]\delta\left(x_3-a\right)\delta\left(x_4-a\right) \tag{3.44}$$

$$\begin{aligned}\langle x_1|\mathbf{G}_Q^o\mathbf{QHPG}_P^o\mathbf{PHQG}_Q^o|x_2\rangle &= \sqrt{\frac{2m}{z\hbar^2}}\sin\left[x_1\sqrt{\frac{2mz}{\hbar^2}}\right]\sin\left[x_2\sqrt{\frac{2mz}{\hbar^2}}\right]\sec\left[a\sqrt{\frac{2mz}{\hbar^2}}\right]^2 \\ &* \cot\left[L\sqrt{\frac{2mz}{\hbar^2}}\right]\end{aligned} \tag{3.45}$$

Letting $\sigma = \sqrt{\frac{2mz}{\hbar^2}}$, we now return to 3.39 to finish computing $\langle x_1|\mathbf{QGQ}|x_2\rangle$:

$$\begin{aligned}&\langle x_1|\mathbf{QGQ}|x_2\rangle = \langle x_1|\mathbf{G}_Q^o|x_2\rangle + \langle x_1|\mathbf{G}_Q^o\mathbf{QHPG}_P^o\mathbf{PHQG}_Q^o|x_2\rangle + \\ &\langle x_1|\mathbf{G}_Q^o\mathbf{QHPG}_P^o\mathbf{PHQ}\left(\mathbf{G}_Q^o\mathbf{QHPG}_P^o\mathbf{PHQ}\right)^1\mathbf{G}_Q^o|x_2\rangle + \ldots + \\ &\langle x_1|\mathbf{G}_Q^o\mathbf{QHPG}_P^o\mathbf{PHQ}\left(\mathbf{G}_Q^o\mathbf{QHPG}_P^o\mathbf{PHQ}\right)^n\mathbf{G}_Q^o|x_2\rangle + \ldots\end{aligned} \tag{3.46}$$

$$\begin{aligned}&= \langle x_1|\mathbf{G}_Q^o|x_2\rangle + \langle x_1|\mathbf{G}_Q^o\mathbf{QHPG}_P^o\mathbf{PHQG}_Q^o|x_2\rangle + \\ &\langle x_1|\mathbf{G}_Q^o\mathbf{QHPG}_P^o\mathbf{PHQG}_Q^o|x_2\rangle\left(\frac{1}{4}\langle a|\mathbf{QHPG}_P^o\mathbf{PHQ}|a\rangle\langle a|\mathbf{G}_Q^o|a\rangle\right) + \ldots + \\ &\langle x_1|\mathbf{G}_Q^o\mathbf{QHPG}_P^o\mathbf{PHQG}_Q^o|x_2\rangle\left(\frac{1}{4}\langle a|\mathbf{QHPG}_P^o\mathbf{PHQ}|a\rangle\langle a|\mathbf{G}_Q^o|a\rangle\right)^n + \ldots\end{aligned} \tag{3.47}$$

$$= \langle x_1|\mathbf{G}_Q^o|x_2\rangle + \langle x_1|\mathbf{G}_Q^o\mathbf{QHPG}_P^o\mathbf{PHQG}_Q^o|x_2\rangle\sum_{n=0}^{\infty}\left(\frac{1}{4}\langle a|\mathbf{QHPG}_P^o\mathbf{PHQ}|a\rangle\langle a|\mathbf{G}_Q^o|a\rangle\right)^n \tag{3.48}$$

$$= \langle x_1|\mathbf{G}_Q^o|x_2\rangle + \frac{\langle x_1|\mathbf{G}_Q^o\mathbf{QHPG}_P^o\mathbf{PHQG}_Q^o|x_2\rangle}{1-\frac{1}{4}\langle a|\mathbf{QHPG}_P^o\mathbf{PHQ}|a\rangle\langle a|\mathbf{G}_Q^o|a\rangle} \tag{3.49}$$

$$= -\frac{\sigma}{z}\frac{\cos\left[\left(a-x_1\right)\sigma\right]\sin\left[x_2\sigma\right]}{\cos\left[a\sigma\right]} + \frac{\sigma}{z}\frac{\cot\left[L\sigma\right]\sec\left[a\sigma\right]^2\sin\left[x_1\sigma\right]\sin\left[x_2\sigma\right]}{1+\cot\left[L\sigma\right]\tan\left[a\sigma\right]} \tag{3.50}$$

$$= -\frac{\sigma}{z}\frac{\sin\left[\left(L+a-x_1\right)\sigma\right]\sin\left[x_2\sigma\right]}{\sin\left[\left(L+a\right)\sigma\right]} \tag{3.51}$$

This is the projected Green's function in the region Q, and as you might expect, it matches the Green's function found in the previous section.

3.6 PGP

Now we'd like to calculate the projected Green's function in region P, **PGP**, and compare it to the projected Green's function in region Q, **QGQ**. Like before, we begin the Green's function solution to Schrödinger's equation:

$$\left(z\mathbf{I}-\mathbf{H}\right)\mathbf{G}\left(z\right)=\mathbf{I} \tag{3.52}$$

and operate with operator $\mathbf{P}$ to the left and right of both sides of the expression to get

$$z\mathbf{PGP}-\mathbf{PHGP}=\mathbf{P}^2=\mathbf{P} \tag{3.53}$$

Next we insert the identity between $\mathbf{H}$ and $\mathbf{G}$, and recalling that $\mathbf{Q}^2=\mathbf{Q}$ and $\mathbf{P}^2=\mathbf{P}$, we write

$$z\mathbf{PGP}-\mathbf{PHPPGP}-\mathbf{PHQQGP}=\mathbf{P} \tag{3.54}$$

thus

$$\mathbf{PGP} = \frac{\mathbf{P}}{z\mathbf{P} - \mathbf{PHP}} + \frac{\mathbf{PHQQGP}}{z\mathbf{P} - \mathbf{PHP}} \tag{3.55}$$

$$= \mathbf{G}_P^o + \mathbf{G}_P^o\mathbf{PHQQGP} \tag{3.56}$$

Returning to 3.52, but this time operating on the left with $\mathbf{Q}$ and on the right with $\mathbf{P}$, we get

$$z\mathbf{QQGP} - \mathbf{QHQQGP} - \mathbf{QHPPGP} = 0 \tag{3.57}$$

Rearranging and inserting 3.56 we find that

$$\mathbf{QGP} = \left(z\mathbf{Q} - \mathbf{QHQ} - \mathbf{QHPG}_P^o\mathbf{PHQ}\right)^{-1}\mathbf{QHPG}_P^o \tag{3.58}$$

Now inserting this back into 3.56, we arrive at the desired result:

$$\mathbf{PGP} = \mathbf{G}_P^o + \mathbf{G}_P^o\mathbf{PHQ}\left(z\mathbf{Q} - \mathbf{QHQ} - \mathbf{QHPG}_P^o\mathbf{PHQ}\right)^{-1}\mathbf{QHPG}_P^o \tag{3.59}$$

$$= \mathbf{G}_P^o + \mathbf{G}_P^o\mathbf{PHQQGQQHPG}_P^o \tag{3.60}$$

Hence (again letting $\sigma = \sqrt{\frac{2mz}{\hbar^2}}$),

$$\langle x_1|\mathbf{PGP}|x_2\rangle = \langle x_1|\mathbf{G}_P^o|x_2\rangle + \langle x_1|\mathbf{G}_P^o\mathbf{PHQQGQQHPG}_P^o|x_2\rangle \tag{3.61}$$

$$= \langle x_1|\mathbf{G}_P^o|x_2\rangle + \int\int dx_3 dx_4 \langle x_1|\mathbf{G}_P^o\mathbf{PHQ}|x_3\rangle\langle x_3|\mathbf{QGQ}|x_4\rangle\langle x_4|\mathbf{QHPG}_P^o|x_2\rangle \tag{3.62}$$

$$= \langle x_1|\mathbf{G}_P^o|x_2\rangle + \left(\frac{\hbar^2}{2m}\right)^2 \partial x_3 \langle x_1|\mathbf{G}_P^o|x_3\rangle\big|_{x_3=a}\langle a|\mathbf{QGQ}|a\rangle\partial x_4\langle x_4|\mathbf{G}_P^o|x_2\rangle\big|_{x_4=a} \tag{3.63}$$

$$= -\frac{\sigma}{z}\frac{\sin\left[(L+a-x_1)\,\sigma\right]\sin\left[(x_2-a)\,\sigma\right]}{\sin\left[L\sigma\right]} - \frac{\sigma}{z}\frac{\sin\left[a\sigma\right]\sin\left[(L+a-x_1)\,\sigma\right]\sin\left[(L+a-x_2)\right]}{\sin\left[L\sigma\right]\sin\left[(L+a)\,\sigma\right]} \tag{3.64}$$

$$= -\frac{\sigma}{z}\frac{\sin\left[(L+a-x_1)\,\sigma\right]\sin\left[x_2\sigma\right]}{\sin\left[(L+a)\,\sigma\right]} \tag{3.65}$$

Note that we have assumed that $x_1 > x_3$ and $x_2 > x_4$. We thus see that $\langle x_1|\mathbf{PGP}|x_2\rangle$ is identical to $\langle x_1|\mathbf{QGQ}|x_2\rangle$ and the spatial matrix elements $\langle x_1|\mathbf{G}|x_2\rangle$ calculated in the previous section.

Chapter 4

Green's Function for a Particle in a 1D Well with a Step Potential

We now add more complexity to the problem by putting a step potential in the region Q (thereby motivating our decision to partition the Green's function in the previous section). Furthermore, we will expand the well into an open quantum system by moving the right hard wall to infinity. This new system is a 1D quantum waveguide with a scattering region at its terminus. We can use this waveguide as a means to investigate properties of various scattering potentials. For example, in the next two sections, we will investigate the step potential's quasibound states as well as scattering particles' survival probabilities within the step potential.

4.1 Problem Setup

The well in consideration is described by the potential (see figure 4.1):

$$V(x) = \begin{cases} \infty & x < 0 \\ V_o & 0 \leq x < a \\ 0 & a \leq x \leq L + a \\ \infty & x > L + a \end{cases} \tag{4.1}$$

When we extend the right wall of the well to infinity, the potential of the system will be (see figure 4.2):

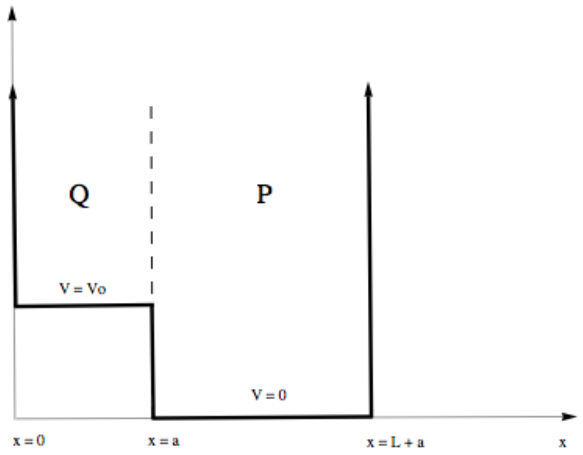

Figure 4.1: 1D Well with Step Potential

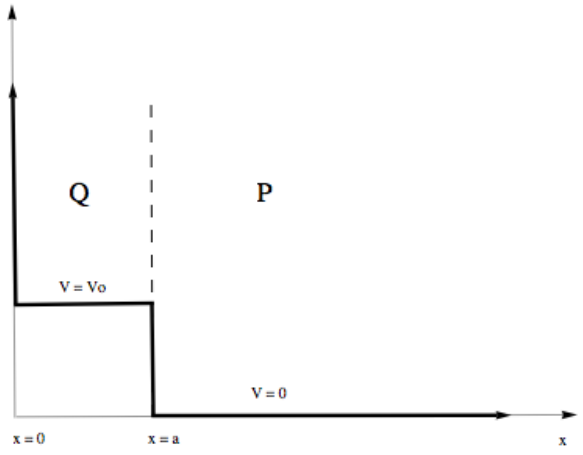

Figure 4.2: 1D Waveguide with Step Potential

$$V(x) = \begin{cases} \infty & x < 0 \\ V_o & 0 \leq x < a \\ 0 & a \leq x < \infty \end{cases} \tag{4.2}$$

4.2 Energy Eigenstates

The boundary conditions and eigenfunctions are the same as in the previous section. Only the eigenvalues are modified by the introduction of a step potential. In Q:

$$\Psi_n^Q = \sqrt{\frac{2}{a}} \sin\left[\frac{(2n-1)\,\pi x}{2a}\right] \tag{4.3}$$

$$E_n^Q = \frac{\hbar^2 \pi^2 (2n-1)^2}{8ma^2} + V_o \tag{4.4}$$

$$n = 1, 2, 3, \ldots \tag{4.5}$$

and in P:

$$\Psi_n^P = \sqrt{\frac{2}{L}} \sin\left[\frac{n\pi\,(x-a)}{L}\right] \tag{4.6}$$

$$E_n^P = \frac{\hbar^2 \pi^2 n^2}{2mL^2} \tag{4.7}$$

$$n = 1, 2, 3, \ldots \tag{4.8}$$

4.3 $\mathbf{G}_Q^o$

Using the eigenfunctions and eigenvalues that we have selected for the region Q, we can calculate $\langle x|\mathbf{G}_Q^o\,(z)\,|x'\rangle$ using the same procedure used previously. If $x_1 > x_2$, then

$$\langle x_1|\mathbf{G}_Q^o(z)|x_2\rangle = -\frac{2m}{\hbar^2}\frac{1}{\sqrt{\frac{2m(z-V_o)}{\hbar^2}}}\frac{\cos\left[(a-x_1)\sqrt{\frac{2m(z-V_o)}{\hbar^2}}\right]\sin\left[x_2\sqrt{\frac{2m(z-V_o)}{\hbar^2}}\right]}{\cos\left[a\sqrt{\frac{2m(z-V_o)}{\hbar^2}}\right]} \tag{4.9}$$

And if $x_2 > x_1$, then

$$\langle x_1|\mathbf{G}_Q^o(z)|x_2\rangle = -\frac{2m}{\hbar^2}\frac{1}{\sqrt{\frac{2m(z-V_o)}{\hbar^2}}}\frac{\cos\left[(a-x_2)\sqrt{\frac{2m(z-V_o)}{\hbar^2}}\right]\sin\left[x_1\sqrt{\frac{2m(z-V_o)}{\hbar^2}}\right]}{\cos\left[a\sqrt{\frac{2m(z-V_o)}{\hbar^2}}\right]} \tag{4.10}$$

4.4 $\mathbf{G}_P^o$

The calculation for $\langle x_1|\mathbf{G}_P^o(z)|x_2\rangle$ is exactly the same as in the previous section. If $x_1 > x_2$, then

$$\langle x_1|\mathbf{G}_P^o(z)|x_2\rangle = -\sqrt{\frac{2m}{z\hbar^2}}\frac{\sin\left[(L+a-x_1)\sqrt{\frac{2mz}{\hbar^2}}\right]\sin\left[(x_2-a)\sqrt{\frac{2mz}{\hbar^2}}\right]}{\sin\left[L\sqrt{\frac{2mz}{\hbar^2}}\right]} \tag{4.11}$$

And if $x_2 > x_1$, then

$$\langle x_1|\mathbf{G}_P^o(z)|x_2\rangle = -\sqrt{\frac{2m}{z\hbar^2}}\frac{\sin\left[(L+a-x_2)\sqrt{\frac{2mz}{\hbar^2}}\right]\sin\left[(x_1-a)\sqrt{\frac{2mz}{\hbar^2}}\right]}{\sin\left[L\sqrt{\frac{2mz}{\hbar^2}}\right]} \tag{4.12}$$

4.5 QGQ

Let $\sigma' = \sqrt{\frac{2m\left(z-V_o\right)}{\hbar^2}}$. We begin our calculation of **QGQ** using the re-summed formula calculated previously:

$$\langle x_1|\mathbf{QGQ}|x_2\rangle = \langle x_1|\mathbf{G}_Q^o|x_2\rangle + \frac{\langle x_1|\mathbf{G}_Q^o\mathbf{QHPG}_P^o\mathbf{PHQG}_Q^o|x_2\rangle}{1-\frac{1}{4}\langle a|\mathbf{QHPG}_P^o\mathbf{PHQ}|a\rangle\langle a|\mathbf{G}_Q^o|a\rangle} \tag{4.13}$$

$$= -\frac{2m}{\sigma'\hbar^2}\left(\frac{\cos\left[\left(a-x_1\right)\sigma'\right]\sin\left[x_2\sigma'\right]}{\cos\left[a\sigma'\right]} - \frac{\sigma}{\sigma'}\frac{\cot\left[L\sigma\right]\sec\left[a\sigma'\right]^2\sin\left[x_1\sigma'\right]\sin\left[x_2\sigma'\right]}{1+\frac{\sigma}{\sigma'}\cot\left[L\sigma\right]\tan\left[a\sigma'\right]}\right) \tag{4.14}$$

$$= -\frac{2m}{\sigma'\hbar^2}\sin\left[x_2\sigma'\right]\left(\frac{\cos\left[\left(a-x_1\right)\sigma'\right]\sin\left[L\sigma\right]+\frac{\sigma}{\sigma'}\sin\left[\left(a-x_1\right)\sigma'\right]\cos\left[L\sigma\right]}{\sin\left[L\sigma\right]\cos\left[a\sigma'\right]+\frac{\sigma}{\sigma'}\sin\left[a\sigma'\right]\cos\left[L\sigma\right]}\right) \tag{4.15}$$

For simplicity, we will only consider the case in which $x_1 > x_2$. If we let $L \to \infty$, turning our well into a quantum waveguide, we see that

$$\langle x_1|\mathbf{QGQ}|x_2\rangle = -\frac{2m}{\sigma'\hbar^2}\sin\left[x_2\sigma'\right]\left(\frac{\cos\left[\left(a-x_1\right)\sigma'\right]-i\frac{\sigma}{\sigma'}\sin\left[\left(a-x_1\right)\sigma'\right]}{\cos\left[a\sigma'\right]-i\frac{\sigma}{\sigma'}\sin\left[a\sigma'\right]}\right) \tag{4.16}$$

$$\begin{aligned} &= -\frac{2m}{\sigma'\hbar^2}\sin\left[x_2\sigma'\right]\left(\frac{\cos\left[\left(a-x_1\right)\sigma'\right]\cos\left[a\sigma'\right]+i\frac{\sigma}{\sigma'}\cos\left[\left(a-x_1\right)\sigma'\right]\sin\left[a\sigma'\right]}{\cos\left[a\sigma'\right]^2+\left(\frac{\sigma}{\sigma'}\right)^2\sin\left[a\sigma'\right]^2}\right)+ \\ &- \frac{2m}{\sigma'\hbar^2}\sin\left[x_2\sigma'\right]\left(\frac{-i\frac{\sigma}{\sigma'}\sin\left[\left(a-x_1\right)\sigma'\right]\cos\left[a\sigma'\right]+\left(\frac{\sigma}{\sigma'}\right)^2\sin\left[\left(a-x_1\right)\sigma'\right]\sin\left[a\sigma'\right]}{\cos\left[a\sigma'\right]^2+\left(\frac{\sigma}{\sigma'}\right)^2\sin\left[a\sigma'\right]^2}\right) \end{aligned} \tag{4.17}$$

4.6 PGP

Using the formula we previously calculated for **PGP**,

$$\langle x_1|\mathbf{PGP}|x_2\rangle = \langle x_1|\mathbf{G}_P^o|x_2\rangle + \left(\frac{\hbar^2}{2m}\right)^2 \partial x_3 \langle x_1|\mathbf{G}_P^o|x_3\rangle\big|_{x_3=a} \langle a|\mathbf{QGQ}|a\rangle \partial x_4 \langle x_4|\mathbf{G}_P^o|x_2\rangle\big|_{x_4=a} \tag{4.18}$$

$$= -\frac{2m}{\sigma\hbar^2}\left(\frac{\sin\left[\left(L+a-x_1\right)\sigma\right]}{\csc\left[\left(x_2-a\right)\sigma\right]\sin\left[L\sigma\right]} + \frac{\sigma}{\sigma'}\frac{\csc\left[L\sigma\right]\sin\left[\left(L+a-x_1\right)\sigma\right]\sin\left[\left(L+a-x_2\right)\sigma\right]}{\sin\left[L\sigma\right]\cot\left[a\sigma'\right]+\frac{\sigma}{\sigma'}\cos\left[L\sigma\right]}\right) \tag{4.19}$$

$$= -\frac{2m}{\sigma\hbar^2}\sin\left[\left(L+a-x_1\right)\sigma\right]\left(\frac{\sin\left[\left(x_2-a\right)\sigma\right]\cos\left[a\sigma'\right]+\frac{\sigma}{\sigma'}\cos\left[\left(x_2-a\right)\sigma\right]\sin\left[a\sigma'\right]}{\sin\left[L\sigma\right]\cos\left[a\sigma'\right]+\frac{\sigma}{\sigma'}\sin\left[a\sigma'\right]\cos\left[L\sigma\right]}\right) \tag{4.20}$$

and when $L \to \infty$,

$$\langle x_1|\mathbf{PGP}|x_2\rangle = -\frac{2m}{\sigma\hbar^2}e^{i(x_1-a)\sigma}\left(\frac{\sin\left[\left(x_2-a\right)\sigma\right]\cos\left[a\sigma'\right]+\frac{\sigma}{\sigma'}\cos\left[\left(x_2-a\right)\sigma\right]\sin\left[a\sigma'\right]}{\cos\left[a\sigma'\right]-i\frac{\sigma}{\sigma'}\sin\left[a\sigma'\right]}\right) \tag{4.21}$$

$$= -\frac{m}{i\sigma\hbar^2}e^{-2ia\sigma}e^{i(x_1+x_2)\sigma}\left(\frac{\cos\left[a\sigma'\right]+i\frac{\sigma}{\sigma'}\sin\left[a\sigma'\right]}{\cos\left[a\sigma'\right]-i\frac{\sigma}{\sigma'}\sin\left[a\sigma'\right]}\right) + \frac{m}{i\sigma\hbar^2}e^{i(x_1-x_2)\sigma} \tag{4.22}$$

$$= -\frac{m}{i\sigma\hbar^2}e^{-2ia\sigma}e^{i(x_1+x_2)\sigma}\left(\frac{1+2i\frac{\sigma}{\sigma'}\tan\left[a\sigma'\right]-\left(\frac{\sigma}{\sigma'}\right)^2\tan\left[a\sigma'\right]^2}{1+\left(\frac{\sigma}{\sigma'}\right)^2\tan\left[a\sigma'\right]^2}\right) \tag{4.23}$$

$$+\frac{m}{i\sigma\hbar^2}e^{i(x_1-x_2)\sigma} \tag{4.24}$$

Again, for simplicity, we will only consider the case in which $x_1 > x_2$.

Chapter 5

Poles and Residues of the Green's Functions for the 1D Well and 1D Waveguide

It is interesting to compare the poles and residues of the the Green's functions for the reaction regions of the well and associated waveguide that we have been discussing. As we will see, the poles of the well are restricted to the real axis of the complex energy plane, whereas the barrier poles have an imaginary component. The well poles are the energy eigenvalues in the well, and their associated resides are the eigenfunctions. The residues of the poles in the waveguide correspond to quasibound states—states that initially resemble the reaction region eigenstates inside the reaction region but leak probability current into the continuum.

In the following analysis, we will use parameter values from [4]. The reaction region is 40 nm long, the step potential is 11.75 x 0.355 meV, and the effective electron mass for a GaAs substrate is 0.067 x 0.51 MeV.

5.1 Well Poles

The poles of 4.15 and 4.20 are found by searching for values of the complex energy $E = S + iT$ for which both the real and imaginary components of the denominator (Δ_W) of 4.15 (or 4.20) are zero:

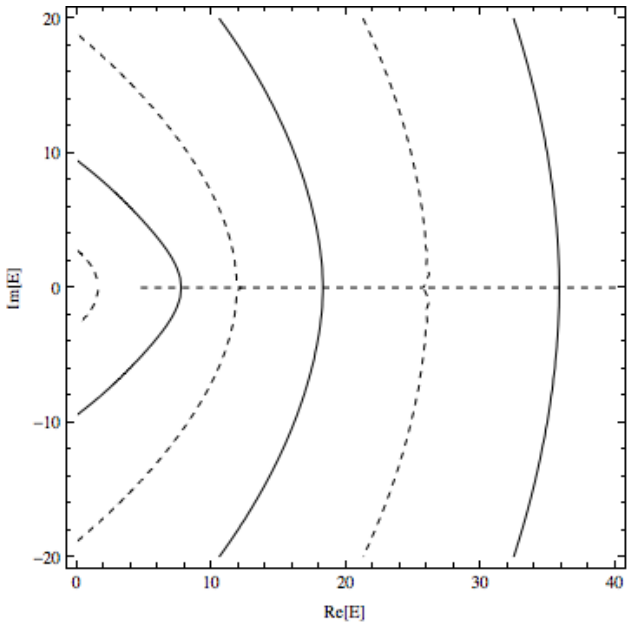

Figure 5.1: Well poles for $L \to 0$. Energy is given in units of meV.

$$\mathrm{Re}\left[\Delta_W\right] = \mathrm{Re}\left[\sin\left[L\sigma\right]\cos\left[a\sigma'\right] + \frac{\sigma}{\sigma'}\sin\left[a\sigma'\right]\cos\left[L\sigma\right]\right] = 0 \tag{5.1}$$

$$\mathrm{Im}\left[\Delta_W\right] = \mathrm{Im}\left[\sin\left[L\sigma\right]\cos\left[a\sigma'\right] + \frac{\sigma}{\sigma'}\sin\left[a\sigma'\right]\cos\left[L\sigma\right]\right] = 0 \tag{5.2}$$

Both 5.1 and 5.2 describe contours in the complex plane. The intersections of these contours are the poles of the system. If $L = 2a$, then we find that the first three intersections are at $\{5.3354, 0\}$, $\{7.7922, 0\}$, and $\{11.1931, 0\}$ meV. If $L \to 0$, the region P is eliminated and the well becomes a square well, the bottom of which is at potential V_o. The first three intersections of 5.1 and 5.2 are then at $\{7.6859, 0\}$, $\{18.2297, 0\}$, and $\{35.8028, 0\}$ meV (see figure 5.1), which are equal to the first three eigenvalues in a square well at potential V_o.

5.2 Waveguide Poles

Similarly, the poles of 4.16 and 4.24 are the values of $E = S + iT$ for which the real and imaginary components of the denominator (Δ_B) of 4.16 (or 4.24) are zero:

$$\mathrm{Re}\left[\Delta_B\right] = \mathrm{Re}\left[\cos\left[a\sigma'\right] - i\left(\frac{\sigma}{\sigma'}\right)\sin\left[a\sigma'\right]\right] = 0 \tag{5.3}$$

$$\mathrm{Im}\left[\Delta_B\right] = \mathrm{Im}\left[\cos\left[a\sigma'\right] - i\left(\frac{\sigma}{\sigma'}\right)\sin\left[a\sigma'\right]\right] = 0 \tag{5.4}$$

The first three intersections between these contours are at {7.0805, -1.6777}, {16.7253, -5.8853}, and {33.5720, -11.4265} meV. Notice that in figure 5.2, the poles for the waveguide barrier have moved off the real axis and into the complex plane. The real parts of these poles are close in value to the poles of the $L \to 0$ well mentioned above.

5.3 Well Residues

The residues of the Green's function in the well give us the eigenfunctions of the system (once again, the contour encloses a single pole p). The Q portion of each eigenfunction is given by:

$$-\left|\Psi_Q\left(x\right)\right|^2 = \mathrm{Res}\left[\langle x|\mathbf{QGQ}|x\rangle\right] = \frac{1}{2\pi i}\int_C \langle x|\mathbf{QGQ}|x\rangle dz \tag{5.5}$$

$$= \lim_{z\to p}\left(z-p\right)\langle x|\mathbf{QGQ}|x\rangle = \lim_{z\to p}\left(z-p\right)\frac{f\left(x,z\right)}{g\left(z\right)} \tag{5.6}$$

$$= \frac{f\left(x,p\right)}{g'\left(p\right)} \tag{5.7}$$

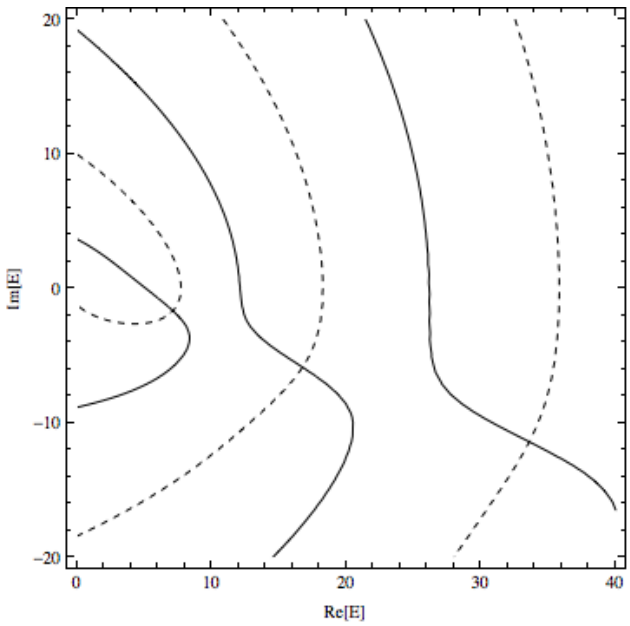

Figure 5.2: Waveguide poles. Energy is given in units of meV.

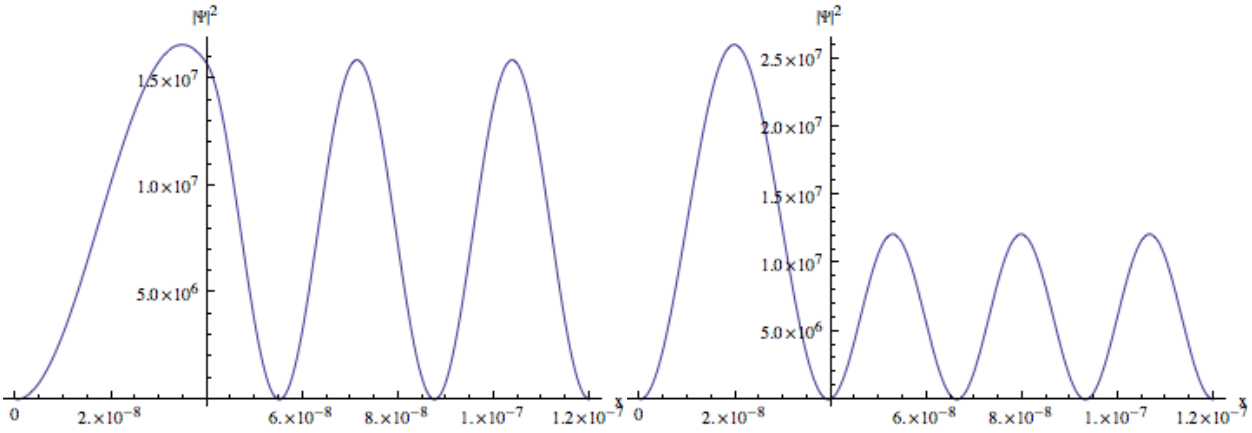

(a) Ground State Probability Distribution (b) First Excited State Probability Distribution

Figure 5.3: These are the first two probability distributions in the $L = 2a$ well. Figure 5.3a corresponds to the pole at p = {5.3354, 0} meV and figure 5.3b corresponds to the pole at p = {7.7922, 0} meV. The well stretches from 0 to 120 nm and the step from 0 to 40 nm.

Equation 5.7 is derived in [15] and is used when $g(z)$ is not easily factorable. A quick glance at equation 4.15 reveals that

$$f(x,z) = -\frac{2m}{\sigma'\hbar^2}\sin[x\sigma']\left(\cos[(a-x)\sigma']\sin[2a\sigma] + \frac{\sigma}{\sigma'}\sin[(a-x)\sigma']\cos[2a\sigma]\right) \tag{5.8}$$

$$g(z) = \sin[2a\sigma]\cos[a\sigma'] + \frac{\sigma}{\sigma'}\sin[a\sigma']\cos[2a\sigma] \tag{5.9}$$

where we have set $L = 2a$. Defining $\sigma_p = \sqrt{\frac{2mp}{\hbar^2}}$ and $\sigma_p' = \sqrt{\frac{2m(p-V_o)}{\hbar^2}}$, we see that

$$|\Psi_Q(x)|^2 = \frac{\frac{2m}{\sigma'\hbar^2}\sin[x\sigma']\left(\cos[(a-x)\sigma']\sin[2a\sigma] + \frac{\sigma}{\sigma'}\sin[(a-x)\sigma']\cos[2a\sigma]\right)}{\frac{ma}{\hbar^2}\left(\frac{2}{\sigma} + \frac{\sigma}{\sigma'^2}\right)\cos[2a\sigma]\cos[a\sigma'] - \frac{3ma}{\sigma'\hbar^2}\sin[2a\sigma]\sin[a\sigma'] - \frac{V_o}{2(z-V_o)^2}\frac{\sigma'}{\sigma}\sin[a\sigma']\cos[2a\sigma]} \tag{5.10}$$

The portion of each eigenfunction that exists in region P is calculated similarly:

$$-|\Psi_P(x)|^2 = \mathrm{Res}\left[\langle x|\mathbf{PGP}|x\rangle\right] = \frac{1}{2\pi i}\int_C \langle x|\mathbf{QGQ}|x\rangle dz \tag{5.11}$$

$$= \lim_{z\to p}(z-p)\langle x|\mathbf{PGP}|x\rangle = \lim_{z\to p}(z-p)\frac{u(x,z)}{v(z)} \tag{5.12}$$

$$= \frac{u(x,p)}{v'(p)} \tag{5.13}$$

with

$$u(x,z) = -\frac{2m}{\sigma\hbar^2}\sin[(L+a-x_1)\sigma]\left(\sin[(x_2-a)\sigma]\cos[a\sigma'] + \frac{\sigma}{\sigma'}\cos[(x_2-a)\sigma]\sin[a\sigma']\right) \tag{5.14}$$

$$v(z) = \sin[2a\sigma]\cos[a\sigma'] + \frac{\sigma}{\sigma'}\sin[a\sigma']\cos[2a\sigma] \tag{5.15}$$

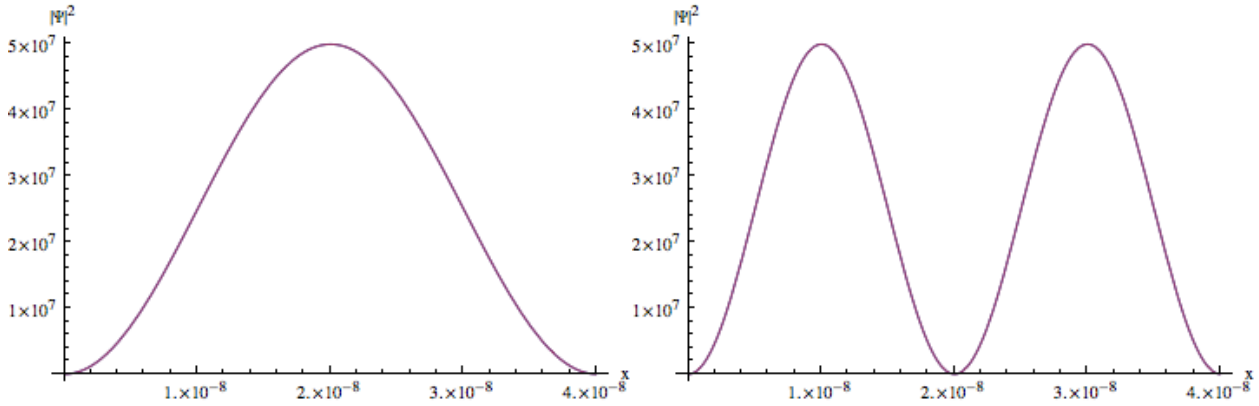

(a) Ground State Probability Distribution (b) First Excited State Probability Distribution

Figure 5.4: These are the first two probability distributions in the $L \to 0$ well. Figure 5.4a corresponds to the pole at p = {7.6859, 0} meV and figure 5.4b corresponds to the pole at p = {18.2297, 0} meV. These agree with the ground state and first excited state probability distributions, respectively, in a square well.

Proceeding, we find that

$$|\Psi_P(x)|^2 = \frac{\frac{2m}{\sigma\hbar^2}\sin[(3a-x_1)\sigma]\sin[(x_2-a)\sigma]\cos[a\sigma'] + \frac{\sigma}{\sigma'}\cos[(x_2-a)\sigma]\sin[a\sigma']}{\frac{ma}{\hbar^2}\left(\frac{2}{\sigma}+\frac{\sigma}{\sigma'^2}\right)\cos[2a\sigma]\cos[a\sigma'] - \frac{3ma}{\sigma'\hbar^2}\sin[2a\sigma]\sin[a\sigma'] - \frac{V_o}{2(z-V_o)^2}\frac{\sigma'}{\sigma}\sin[a\sigma']\cos[2a\sigma]} \tag{5.16}$$

The first two residues in the well are graphed in figure 5.3. Notice that the particle wavelength shrinks outside the step, where the particle has more kinetic energy and therefore a higher wave number.

Using the poles for the $L \to 0$ well case, we repeated the above calculation with $L = 0$ to demonstrate that we can recover the eigenstates of a square well using residues. This is shown in figure 5.4.

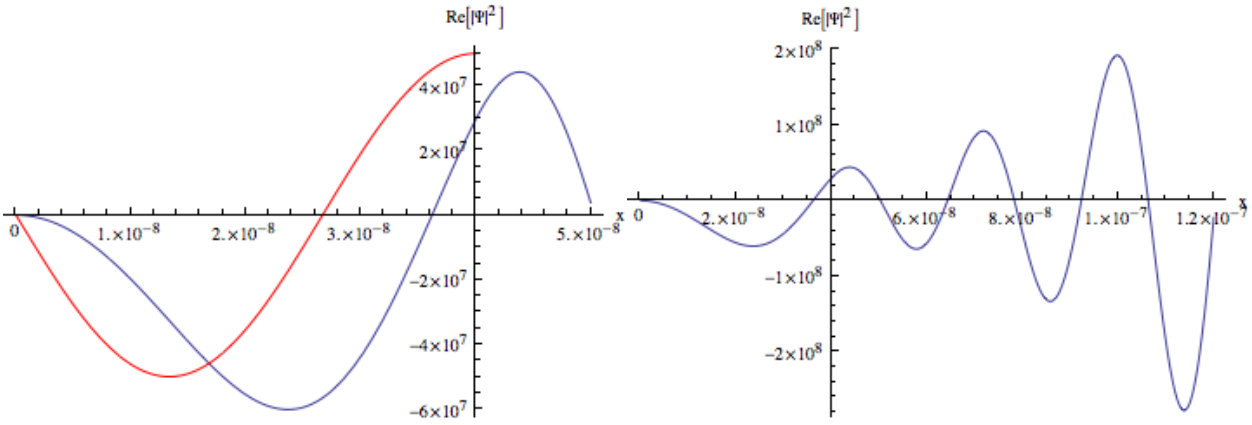

(a) First Quasibound State in Reaction Region

(b) First Quasibound State

Figure 5.5: The first quasibound state probability distribution is shown here. In figure 5.5a, the first excited state energy eigenfunction in the reaction region is shown for comparison. As shown in figure 5.5b, the first quasibound state loses meaning and significance far from the reaction region.

5.4 Waveguide Residues

The residues of the Green's function for the barrier region of the waveguide give us the Q portion of the quasibound states in the open system:

$$-|\Psi_Q(x)|^2 = \text{Res}\left[\langle x|\mathbf{QGQ}|x\rangle\right] = \frac{1}{2\pi i}\int_C \langle x|\mathbf{QGQ}|x\rangle dz \tag{5.17}$$

$$= \lim_{z\to p}(z-p)\langle x|\mathbf{QGQ}|x\rangle = \lim_{z\to p}(z-p)\frac{F(x,z)}{G(z)} \tag{5.18}$$

$$= \frac{F(x,p)}{G'(p)} \tag{5.19}$$

Comparing 5.24 with 4.16, we see that

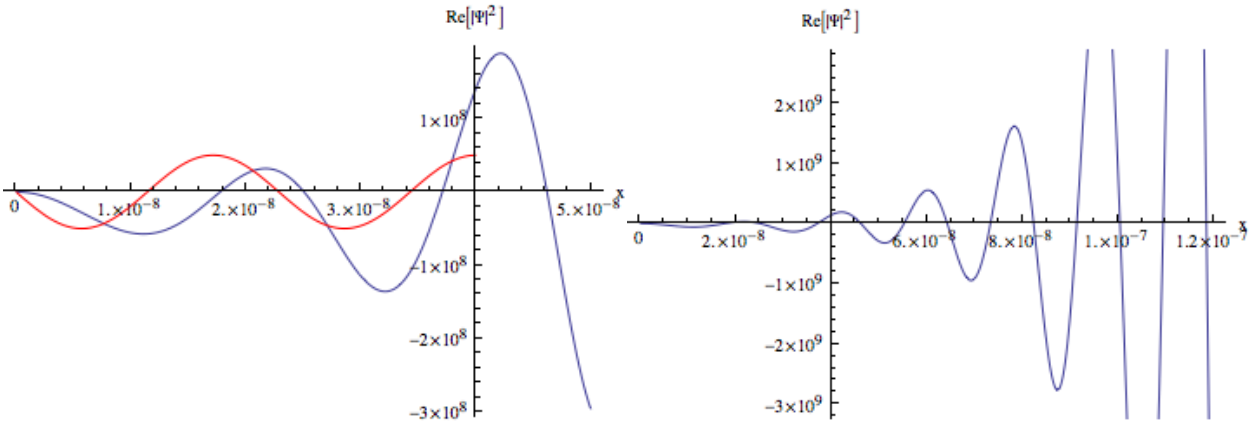

(a) Second Quasibound State in Reaction Region (b) Second Quasibound State

Figure 5.6: These figures show the second quasibound state probability distribution. In figure 5.6a, the third excited state energy eigenfunction in the reaction region is shown for comparison. As shown in figure 5.6b, the second quasibound state loses meaning and significance far from the reaction region.

$$F(x,z) = -\frac{2m}{\sigma'\hbar^2}\sin[x_2\sigma']\left(\cos[(a-x_1)\sigma'] - i\frac{\sigma}{\sigma'}\sin[(a-x_1)\sigma']\right) \tag{5.20}$$

$$G(z) = \cos[a\sigma'] - i\frac{\sigma}{\sigma'}\sin[a\sigma'] \tag{5.21}$$

Hence,

$$-|\Psi_Q(x)|^2 = \frac{2m}{\sigma'\hbar^2}\sin[x_2\sigma']\frac{\cos[(a-x_1)\sigma'] - i\frac{\sigma}{\sigma'}\sin[(a-x_1)\sigma']}{-\frac{ma}{\sigma'\hbar^2}\sin[a\sigma'] + i\left(\frac{V_o}{2(z-V_o)^2}\frac{\sigma'}{\sigma}\sin[a\sigma'] + \frac{ma}{\sigma'\hbar^2}\frac{\sigma}{\sigma'}\cos[a\sigma']\right)} \tag{5.22}$$

Likewise, in P:

$$-|\Psi_P(x)|^2 = \mathrm{Res}\left[\langle x|\mathbf{PGP}|x\rangle\right] = \frac{1}{2\pi i}\int_C \langle x|\mathbf{PGP}|x\rangle dz \tag{5.23}$$

$$= \lim_{z\to p}(z-p)\,\langle x|\mathbf{PGP}|x\rangle = \lim_{z\to p}(z-p)\,\frac{U(x,z)}{V(z)} \tag{5.24}$$

$$= \frac{U(x,p)}{V'(p)} \tag{5.25}$$

with

$$U(x,z) = -\frac{2m}{\sigma\hbar^2}e^{i(x_1-a)\sigma}\left(\sin\left[(x_2-a)\,\sigma\right]\cos\left[a\sigma'\right] + \frac{\sigma}{\sigma'}\cos\left[(x_2-a)\,\sigma\right]\sin\left[a\sigma'\right]\right) \tag{5.26}$$

$$V(z) = \cos\left[a\sigma'\right] - i\frac{\sigma}{\sigma'}\sin\left[a\sigma'\right] \tag{5.27}$$

and therefore

$$|\Psi_P(x)|^2 = \frac{2m}{\sigma\hbar^2}e^{i(x_1-a)\sigma}\frac{\left(\sin\left[(x_2-a)\,\sigma\right]\cos\left[a\sigma'\right] + \frac{\sigma}{\sigma'}\cos\left[(x_2-a)\,\sigma\right]\sin\left[a\sigma'\right]\right)}{-\frac{ma}{\sigma'\hbar^2}\sin\left[a\sigma'\right] + i\left(\frac{V_o}{2(z-V_o)^2}\frac{\sigma'}{\sigma}\sin\left[a\sigma'\right] + \frac{ma}{\sigma'\hbar^2}\frac{\sigma}{\sigma'}\cos\left[a\sigma'\right]\right)} \tag{5.28}$$

The first two quasibound state probability distributions are graphed in figures 5.5 and 5.6. Two important features to note are their particular deviations from their associated reaction region eigenstates (included in the figures for comparison) and their behavior far from the reaction region. The reaction region eigenstates are normalizable, but the quasibound states are not—they blow up as $x \to \infty$. This phenomenon is well known and is the basis for rigged Hilbert space.

Chapter 6

Survival Probabilities of Particles in the Reaction Region of the 1D Waveguide

In this section, we compute the likelihood that a particle will remain in the reaction region once placed there over time. The reaction region in consideration will be the same as the one described in chapter four—namely, a step potential extending from $x = 0$ nm to $x = 40$ nm inside a waveguide. We will consider a Gaussian initial particle state for demonstration purposes.

6.1 Gaussian Initial State

Recalling that $z = E + i\delta$, the survival probability ($A_\psi(t)$) of a scattering particle can be computed using the inverse Laplace transform [5]:

$$A_\psi(t) = \int dz e^{-\frac{i}{\hbar}zt} \langle\psi|\mathbf{QGQ}|\psi\rangle \tag{6.1}$$

$$= \int \int_0^a \int_0^a dz dx_1 dx_2 e^{-izt} \langle\psi|x_1\rangle\langle x_1|\mathbf{QGQ}|x_2\rangle\langle x_2|\psi\rangle \tag{6.2}$$

We take $\psi(x_1)$ and $\psi(x_2)$ to be normalized Gaussians of the form $\left(\frac{2c}{\pi}\right)^{1/4} e^{-c\left(x-\frac{a}{2}\right)^2}$, with $c = \left(\frac{10}{a}\right)^2$. Hence,

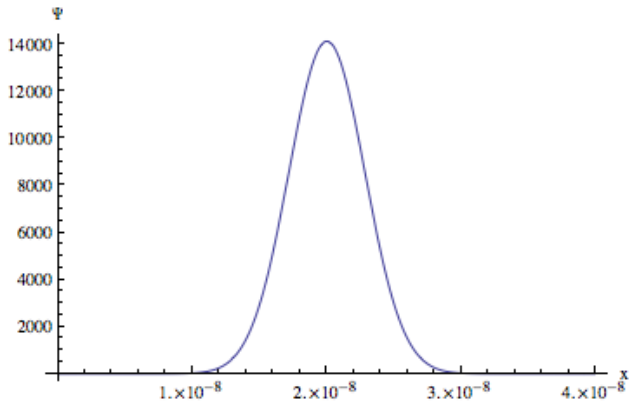

Figure 6.1: Gaussian Initial Particle State. Notice its positioning about the center of the reaction region and its negligible amplitude outside the reaction region. x is measured in meters and is the distance from the left wall of the waveguide.

$$A_\psi(t) = \int_0^a \int_0^a dx_1 dx_2 \left(\frac{2c}{\pi}\right)^{1/2} e^{-c\left(x_1-\frac{a}{2}\right)^2} e^{-c\left(x_2-\frac{a}{2}\right)^2} \frac{i}{2\pi} \oint_C e^{-\frac{i}{\hbar}zt} \langle x_1|\mathbf{QGQ}|x_2\rangle \tag{6.3}$$

$$= -\int_0^a \int_0^a dx_1 dx_2 \left(\frac{2c}{\pi}\right)^{1/2} e^{-c\left(x_1-\frac{a}{2}\right)^2} e^{-c\left(x_2-\frac{a}{2}\right)^2} \sum \text{Res}\left[e^{-\frac{i}{\hbar}zt} \langle x_1|\mathbf{QGQ}|x_2\rangle\right] \tag{6.4}$$

where we have used the Cauchy residue theorem. The contour of integration runs from $(-\infty, i\delta)$ to $(\infty, i\delta)$ and is closed clockwise in the lower half plane. These selections are required by the forward arrow of time. Note that the poles of 6.4 are the same as those of $\langle x_1|\mathbf{QGQ}|x_2\rangle$ calculated in the previous section. The residues are the quasibound states multiplied by the decay factor $e^{-\frac{i}{\hbar}zt}$. There are an infinite number of poles in an open system, but we only include the first dozen in this particular example, since the overlap of the residues with a Gaussian initial state is highest for lower order energy modes—e.g., the real part of the eleventh residues' contribution to $A_\psi(t)$ is less than a thousandth of the real part of the first residues' contribution.

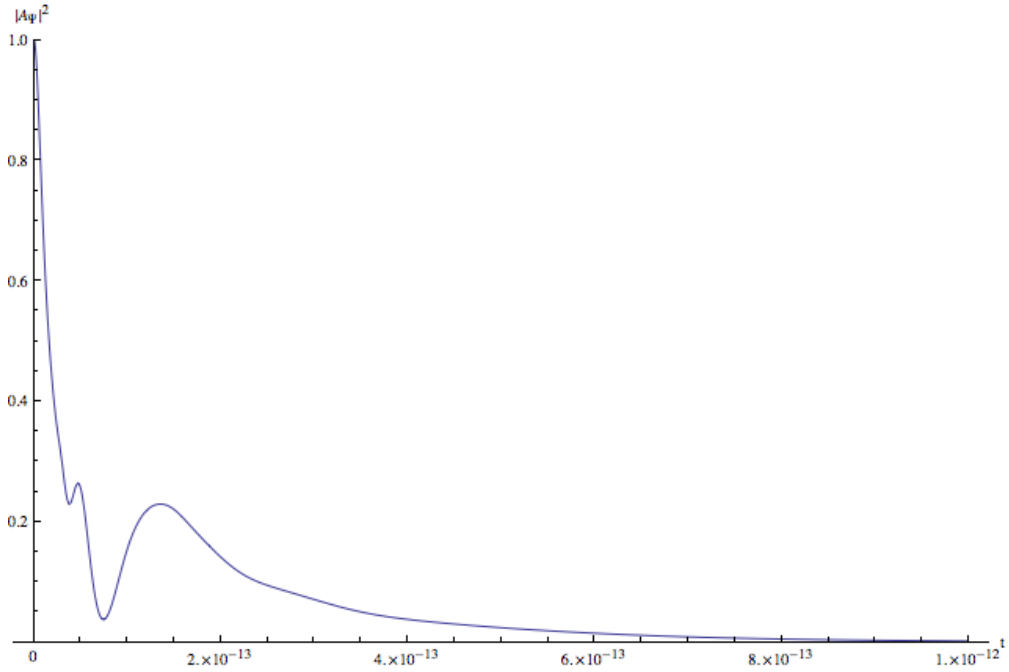

Figure 6.2: Survival Probability for a Gaussian initial particle state. Time is given in seconds.

The survival probability, $|A_\psi|^2$, is graphed in figure 6.2. Its oscillatory behavior can be attributed to the composition of a Gaussian. Its overlap with each of the quasibound states varies in magnitude, and the sum of these overlaps generates the unique curve shown.

Chapter 7

Calculating the S-matrix for a 1D Step Potential from the Green's Function

The S-matrix is useful for storing reflection and transmission amplitudes for incoming asymptotic scattering waves. It's especially useful for problems in higher dimensions with multiple energy channels within two or more waveguide leads. In the case of a single lead in one dimension however, the S-matrix merely consists of a single element—the reflection amplitude. It turns out that the S-matrix can be constructed using the Green's function for a system. In this section, we will demonstrate how to get the reflection amplitude from the Green's function of an incoming matter wave inside a waveguide with a step against a hard wall at one end.

7.1 Limiting form of $\mathbf{G}_P^o$

The S-matrix is used for open scattering systems. Since we will be using $\mathbf{G}_P^o$ later in our calculations, we compute the limit of 4.11 in which $L \to \infty$ here.

$$\lim_{L\to\infty} \langle x_1|\mathbf{G}_P^o|x_2\rangle = -\frac{m}{i\sigma\hbar^2}\left(e^{-2ia\sigma}e^{i(x_2+x_1)\sigma} - e^{-i(x_2-x_1)\sigma}\right) \tag{7.1}$$

An important note: to calculate the reflection amplitude for this scattering process, we only want the component of the Green's function that would time-evolve a particle wave

function from x_1 to x_2 via reflection off the step potential and hard wall. The distance covered by the particle would be $x_1 + x_2$, so we neglect the alternative process in which the wave is simply propagated directly from x_1 to x_2 and write

$$\langle x_1|\mathbf{G}_P^o|x_2\rangle = -\frac{m}{i\sigma\hbar^2}e^{-2ia\sigma}e^{i(x_2+x_1)\sigma} \tag{7.2}$$

7.2 PGP Revisited

In this section, we recast 3.59 in a form that will allow us to directly associate the Green's function with an expression for the reflection amplitude in a 1D S-matrix. This calculation follows the steps outlined in Reichl's *Transition to Chaos* [14]. We begin with a spatial matrix element of 3.59:

$$\langle x_1|\mathbf{PGP}|x_2\rangle = \langle x_1|\mathbf{G}_P^o|x_2\rangle + \langle x_1|\mathbf{G}_P^o\mathbf{PHQ}\left(z\mathbf{Q} - \mathbf{QHQ} - \mathbf{QHPG}_P^o\mathbf{PHQ}\right)^{-1}\mathbf{QHPG}_P^o|x_2\rangle \tag{7.3}$$

$$= \langle x_1|\mathbf{G}_P^o|x_2\rangle +$$
$$\int\int dx_3dx_4\langle x_1|\mathbf{G}_P^o\mathbf{PHQ}|x_3\rangle\langle x_3|\mathbf{Q}\left(z\mathbf{Q} - \mathbf{QHQ} - \mathbf{QHPG}_P^o\mathbf{PHQ}\right)^{-1}\mathbf{Q}|x_4\rangle \tag{7.4}$$
$$* \langle x_4|\mathbf{QHPG}_P^o|x_2\rangle$$

Using 7.2, we can write

$$\langle x_1|\mathbf{G}_P^o\mathbf{PHQ}|x_3\rangle = e^{-ia\sigma}e^{ix_1\sigma}\delta\left(x_3 - a\right) \tag{7.5}$$

$$\langle x_4|\mathbf{QHPG}_P^o|x_2\rangle = e^{-ia\sigma}e^{ix_2\sigma}\delta\left(x_4 - a\right) \tag{7.6}$$

Now let us consider the inner bracket in 7.4. Using the completeness of the eigenstates in the reaction region (but limiting the number of states to large N rather than infinity for computational purposes), we can write

$$\begin{aligned}&\mathbf{Q}\left(z\mathbf{Q}-\mathbf{QHQ}-\mathbf{QHPG}_P^o\mathbf{PHQ}\right)^{-1}\mathbf{Q}=\\&\sum_{i,j=1}^{N}\mathbf{Q}|\phi_i\rangle\langle\phi_i|\left(z\mathbf{Q}-\mathbf{QHQ}-\mathbf{QHPG}_P^o\mathbf{PHQ}\right)^{-1}|\phi_j\rangle\langle\phi_j|\mathbf{Q}\end{aligned}\tag{7.7}$$

$\left(z\mathbf{Q}-\mathbf{QHQ}-\mathbf{QHPG}_P^o\mathbf{PHQ}\right)^{-1}$ can be expanded, operated on the left with $\langle\phi_i|$ and on the right with $|\phi_j\rangle$, and then re-summed and converted back into a matrix. The calculation is equivalent to computing $\langle\phi_i|z\mathbf{Q}-\mathbf{QHQ}-\mathbf{QHPG}_P^o\mathbf{PHQ}|\phi_j\rangle$, converting the result into a matrix, and then taking the inverse of this matrix. $\langle\phi_i|\mathbf{QHPG}_P^o\mathbf{PHQ}|\phi_j\rangle$ is computed as follows:

$$\langle\phi_i|\mathbf{QHPG}_P^o\mathbf{PHQ}|\phi_j\rangle=\int_a^\infty\int_a^\infty dx_5dx_6\langle\phi_i|\mathbf{QHP}|x_5\rangle\langle x_5|\mathbf{G}_P^o|x_6\rangle\langle x_6|\mathbf{PHQ}|\phi_j\rangle \tag{7.8}$$

$$=\left(-\frac{2\hbar^2}{m}\right)^2\int_a^\infty\int_a^\infty dx_5dx_6\phi_i\left(x_5\right)\delta\left(x_5-a\right)\partial x_5\partial x_6\langle x_5|\mathbf{G}_P^o|x_6\rangle\phi_j\left(x_6\right)\delta\left(x_6-a\right) \tag{7.9}$$

$$=-i\frac{\hbar^2\sigma}{2m}\phi_i\left(a\right)\phi_j\left(a\right) \tag{7.10}$$

$$=-i\omega_i\omega_j \tag{7.11}$$

where we have defined $\omega_i=\sqrt{\frac{\hbar^2\sigma}{2m}}\phi_i\left(a\right)$. This allows us to write $\langle\phi_i|z\mathbf{Q}-\mathbf{QHQ}-\mathbf{QHPG}_P^o\mathbf{PHQ}|\phi_j\rangle$ as follows:

$$\langle\phi_i|z\mathbf{Q}-\mathbf{QHQ}-\mathbf{QHPG}_P^o\mathbf{PHQ}|\phi_j\rangle = (z-\lambda_i)\,\delta_{i,j}+i\omega_i\omega_j \tag{7.12}$$

$$= \left(z\mathbf{I}-\mathbf{H}_{in}+i\boldsymbol{\omega}\boldsymbol{\omega}^T\right)_{i,j} \tag{7.13}$$

Using the orthogonality and completeness of the reaction region basis states, $\mathbf{Q}|\phi_i\rangle$, we can now write

$$\mathbf{Q}\left(z\mathbf{Q}-\mathbf{QHQ}-\mathbf{W}\right)^{-1}\mathbf{Q} = \mathbf{Q}\left(|\phi\rangle\right)^T\left(z\mathbf{I}-\mathbf{H}_{in}+i\boldsymbol{\omega}\boldsymbol{\omega}^T\right)^{-1}\left(\langle\phi|\right)\mathbf{Q} \tag{7.14}$$

where $\langle\phi|$ denotes a column vector of cavity basis states:

$$\langle\phi| = \begin{pmatrix} \langle\phi_1| \\ \vdots \\ \langle\phi_N| \end{pmatrix} \tag{7.15}$$

$$\left(|\phi\rangle\right)^T = \begin{pmatrix} |\phi_1\rangle, & \ldots, & |\phi_N\rangle \end{pmatrix} \tag{7.16}$$

Combining equations 7.14, 7.5, and 7.6, we see that

$$\langle x_1|\mathbf{PGP}|x_2\rangle = -\frac{-m}{i\sigma\hbar^2}e^{-2ia\sigma}e^{i(x_1+x_2)\sigma}\left(1-2i\boldsymbol{\omega}^T\frac{1}{z\mathbf{I}-\mathbf{H}_{in}+i\boldsymbol{\omega}\boldsymbol{\omega}^T}\boldsymbol{\omega}\right) \tag{7.17}$$

where

$$\boldsymbol{\omega} = \begin{pmatrix} \omega_1 \\ \vdots \\ \omega_N \end{pmatrix} \tag{7.18}$$

$$\boldsymbol{\omega}^T = \begin{pmatrix} \omega_1, & \ldots, \omega_N \end{pmatrix} \tag{7.19}$$

7.3 Reflection Amplitude

The S-matrix (reflection amplitude) for a 1D waveguide consisting of a single lead with a single channel and a step potential ending at $x = a$ can be expressed as follows (see section 8):

$$S = R(z) = e^{-2ia\sigma}\left(1 - 2i\boldsymbol{\omega}^T \frac{1}{z\mathbf{I} - \mathbf{H}_{in} + i\boldsymbol{\omega}\boldsymbol{\omega}^T}\boldsymbol{\omega}\right) \tag{7.20}$$

If we compare this to equation 7.17, we see that

$$S = R(z) = \frac{-i\sigma\hbar^2}{m} e^{-i(x_1+x_2)\sigma} \langle x_1|\mathbf{PGP}|x_2\rangle \tag{7.21}$$

Now, for the open waveguide, recall that

$$\begin{aligned} \langle x_1|\mathbf{PGP}|x_2\rangle = &- \frac{m}{i\sigma\hbar^2} e^{-2ia\sigma} e^{i(x_1+x_2)\sigma} \left(\frac{1 + 2i\frac{\sigma}{\sigma'}\tan\left[a\sigma'\right] - \left(\frac{\sigma}{\sigma'}\right)^2 \tan\left[a\sigma'\right]^2}{1 + \left(\frac{\sigma}{\sigma'}\right)^2 \tan\left[a\sigma'\right]^2}\right) + \\ &\frac{m}{i\sigma\hbar^2} e^{i(x_1-x_2)\sigma} \end{aligned} \tag{7.22}$$

Like we did with $\mathbf{G}_P^o$, we take the term that includes reflection off the step potential and hard wall to write

$$\langle x_1|\mathbf{PGP}|x_2\rangle = -\frac{m}{i\sigma\hbar^2}e^{-2ia\sigma}e^{i(x_1+x_2)\sigma}\left(\frac{1+2i\frac{\sigma}{\sigma'}\tan\left[a\sigma'\right]-\left(\frac{\sigma}{\sigma'}\right)^2\tan\left[a\sigma'\right]^2}{1+\left(\frac{\sigma}{\sigma'}\right)^2\tan\left[a\sigma'\right]^2}\right) \tag{7.23}$$

$$= -\frac{m}{i\sigma\hbar^2}e^{-2ia\sigma}e^{i(x_1+x_2)\sigma}e^{2i\arctan\left(\frac{\sigma}{\sigma'}\tan[a\sigma']\right)} \tag{7.24}$$

Substituting this simplified expression for $\langle x_1|\mathbf{PGP}|x_2\rangle$ into 7.21, we can finally write

$$S = R\left(z\right) = e^{-2ia\sigma}e^{2i\arctan\left(\frac{\sigma}{\sigma'}\tan[a\sigma']\right)} \tag{7.25}$$

Chapter 8

Reaction Function Methods

In this section we will use R-matrix theory to calculate the S-matrix and the poles for a step potential against a hard wall.

8.1 Reaction Function Definition

Following the steps outlined in Reichl's *Transition to Chaos* [14], we compute the reaction function for the potential barrier in section four. We begin with the general form of the reaction function for a 1D system:

$$R(E) = \frac{\hbar^2}{2m} \sum_{n=1}^{\infty} \frac{\phi_n^2(a)}{E - \lambda_n} \tag{8.1}$$

We choose the same eigenfunctions and eigenvalues as before

$$\phi_n^Q = \sqrt{\frac{2}{a}} \sin\left[\frac{(2n-1)\pi x}{2a}\right] \tag{8.2}$$

$$\lambda_n^Q = \frac{\hbar^2 \pi^2 (2n-1)^2}{8ma^2} + V_o \tag{8.3}$$

$$n = 1, 2, 3, \ldots \tag{8.4}$$

So that

$$R(E) = \frac{\hbar^2}{2m} \sum_{n=1}^{\infty} \frac{\sin\left[\frac{(2n-1)\pi}{2}\right]^2}{E - \frac{\hbar^2\pi^2(2n-1)^2}{8ma^2} - V_o} \tag{8.5}$$

Let $\kappa^2 = \dfrac{2mV_o}{\hbar^2}$, $k^2 = \dfrac{2mE}{\hbar^2}$, and $k'^2 = \dfrac{2m(E-V_o)}{\hbar^2}$, then

$$R(E) = \frac{2}{a^2} \sum_{n=1}^{\infty} \frac{1}{k^2 - \kappa^2 - \frac{\pi^2(2n-1)^2}{4a^2}} = \frac{\tan\left[\sqrt{k^2-\kappa^2}a\right]}{\sqrt{k^2-\kappa^2}a} = \frac{\tan(k'a)}{k'a} \tag{8.6}$$

where we have used formula 6.1.41 on page 104 of Hansen's *A Table of Series and Products* [16] for the sum. This is the reaction function for the 1D step potential against a hard wall.

8.2 Calculating the S-Matrix from the Reaction Function

We can calculate the scattering matrix directly from the reaction function. In general [14],

$$\mathbf{S} = \mathbf{U}_k^{\dagger} \frac{\mathbf{I} - i\mathbf{K}}{\mathbf{I} + i\mathbf{K}} \mathbf{U}_k^{\dagger} \tag{8.7}$$

where

$$K_{\alpha\beta(n,n')} = \sqrt{k_n} R_{\alpha\beta} \sqrt{k_{n'}} \tag{8.8}$$

$$U_{n,n'} = e^{ik_n a} \delta_{n,n'} \tag{8.9}$$

But since we're working in 1D with a single channel,

$$S(E) = e^{-2ika}\frac{1+ikaR(E)}{1-ikaR(E)} \tag{8.10}$$

$$= e^{-2ika}e^{2i\arctan\left(\frac{k}{k'}\tan[k'a]\right)} \tag{8.11}$$

where $k = \sqrt{\frac{2mE}{\hbar^2}}$ and $k' = \sqrt{\frac{2m(E-V_o)}{\hbar^2}}$. If we let $E \to z = E + i\delta$, then $k \to \sigma$ and $k' \to \sigma'$, and we recover the same S-matrix we calculated using the Green's function for this system.

8.3 Re-summing the S-matrix

8.7 can be re-summed to take the form (see Appendix, section 10.4):

$$\mathbf{S} = \mathbf{U}_k^\dagger \left(\mathbf{I} - 2i\boldsymbol{\omega}^T \frac{1}{E\mathbf{I} - \mathbf{H}_{in} + i\boldsymbol{\omega}\boldsymbol{\omega}^T}\boldsymbol{\omega}\right)\mathbf{U}_k^\dagger \tag{8.12}$$

where we restrict the number of reaction region eigenvalues to N, such that H_{in} is an NxN diagonal matrix:

$$H_{in} = \begin{pmatrix} \lambda_1 & 0 & \dots & 0 \\ 0 & \lambda_2 & \dots & 0 \\ \vdots & \vdots & \ddots & \vdots \\ 0 & 0 & \dots & \lambda_N \end{pmatrix} \tag{8.13}$$

$\boldsymbol{\omega}$ is an NxM coupling matrix:

$$w_{j,n} = \phi_{j,n}(a)\sqrt{\frac{\hbar^2 k_n}{2m}} \tag{8.14}$$

which, in our single channel ($M = 1$) case, is

$$\boldsymbol{\omega} = \sqrt{\frac{\hbar^2 k}{2m}} \begin{pmatrix} \phi_1(a) \\ \phi_2(a) \\ \vdots \\ \phi_N(a) \end{pmatrix} = \sqrt{\frac{\hbar^2 k}{2m}} \sqrt{\frac{2}{a}} \begin{pmatrix} 1 \\ -1 \\ \vdots \\ -1\,(1) \end{pmatrix} \tag{8.15}$$

8.4 Poles of the S-matrix

Looking at equation 8.12, we immediately recognize that the poles of the S-matrix are the eigenvalues of the effective Hamiltonian

$$\mathbf{H}_{eff} = \mathbf{H}_{in} - i\boldsymbol{\omega}\boldsymbol{\omega}^T \tag{8.16}$$

which we determine by finding the values of E in ω for which

$$\mathrm{Det}\left[\mathbf{H}_{in} - i\boldsymbol{\omega}\boldsymbol{\omega}^T\right] = 0 \tag{8.17}$$

These values are determined iteratively by guessing a complex value for E and then comparing it against the computed eigenvalues from 8.17. If they are different, a new guess must be made and the process repeated. Note that N must be sufficiently large for a given energy eigenvalue to converge to its true ($N = \infty$) value. As a test, we we compared the first three actual poles (determined graphically in section 5.2) with the complex energy eigenvalues computed via the method described here. The results are given in table 8.1,

where N refers to the dimension of the complex Hamiltonian (limited for computational purposes).

Table 8.1: Numerical comparisons of Poles

Actual Pole (meV)	$N = 5000$	$N = 10000$
$7.08054 - 1.67777i$	$7.0807 - 1.6782i$	$7.08064 - 1.67796i$
$16.7253 - 5.88537i$	$16.7264 - 5.8890i$	$16.7259 - 5.8872i$
$33.5720 - 11.4265i$	$33.5756 - 11.4414$	$33.5738 - 11.4339i$

Chapter 9

Conclusion

The primary aim of this paper has been to demonstrate the usefulness and versatility of the Green's function in quantum waveguides. Its connection to the propagator makes the Green's function ideally suited for calculating the S-matrix for a scattering process. With this comes the usual fruits of the S-matrix—poles and transmission and reflection amplitudes. However, because it is more general, the Green's function yields other useful information, including particle eigenstates for closed systems, or quasibound states for open systems, and particle survival probabilities. We have also shown that we can derive the S-matrix and poles for a system using R-matrix theory. However, R-matrix theory does not give us quasibound states or particle survival probabilities.

We have illustrated a number of Green's functions calculations for the simple case of a 1D step potential against a hard wall. This system was chosen for its simplicity, but the methods outlined in this paper are easily generalizable to higher dimensions and additional waveguide leads. One begins with a bounded system that is divided into regions with different potentials. If a complete set of discrete energy eigenstates subject to Wigner-Eisenbud boundary conditions can be written down for each region, then the Green's function for that region can be constructed. The Green's function for each region is then singularly coupled to its neighboring regions. This completes the calculation of the Green's function for the

entire bounded system. The Green's function for the corresponding open system is found by analytic continuation of the Green's function ($L \to \infty$). From this we can get an S-matrix, quasibound states, and survival probabilities.

If extended to two dimensions, this method yields theoretical results to which experimental nanoscale electron waveguide data can be compared. Furthermore, the scattering properties of more complicated potentials could be studied in isolation, a particular advantage conferred by combining waveguides and reaction regions.

Appendix

10.1 Summation Formula for 2.17

To compute the sum in 2.17, we rely on formula 17.3.9 found on p. 243 of Hansen's *A Table of Series and Products* [16]:

$$\sum_{n=1}^{\infty} \frac{\cos\left[nx\right)}{n^2d^2 - b^2} = \frac{1}{2b^2} - \frac{\pi}{2db}\cos\left[\left[(2m+1)\,\pi - x\right]\frac{b}{d}\right]\csc\left[\frac{\pi b}{d}\right] \tag{10.1}$$

where m is an integer, $\dfrac{b}{d}$ is not an integer, and $2\pi m \leq x \leq 2\pi\,(m+1)$.

First consider the cosine term in 2.17 that includes $(x_1 - x_2)$ in its argument. In our case, we choose Hansen's x to be $\dfrac{(x_1 - x_2)\,\pi}{L+a}$ (requiring that $x_1 > x_2$), $d = \dfrac{\pi}{(L+a)}$, $b = \sqrt{\dfrac{2mz}{\hbar^2}}$, and $m = 0$, giving

$$\sum_{n=1}^{\infty} \frac{\cos\left[\frac{n\pi(x_1-x_2)}{L+a}\right]}{\frac{n^2\pi^2}{(L+a)^2} - \frac{2mz}{\hbar^2}} = \frac{\hbar^2}{4mz} - \frac{L+a}{2}\sqrt{\frac{\hbar^2}{2mz}}\cos\left[(L+a+x_2-x_1)\sqrt{\frac{2mz}{\hbar^2}}\right]\csc\left[(L+a)\sqrt{\frac{2mz}{\hbar^2}}\right] \tag{10.2}$$

Similarly, the second cosine in the sum can be written

$$\sum_{n=1}^{\infty} \frac{\cos\left[\frac{n\pi(x_1+x_2)}{L+a}\right]}{\frac{n^2\pi^2}{(L+a)^2} - \frac{2mz}{\hbar^2}} = \frac{\hbar^2}{4mz} - \frac{L+a}{2}\sqrt{\frac{\hbar^2}{2mz}}\cos\left[(L+a-x_2-x_1)\sqrt{\frac{2mz}{\hbar^2}}\right]\csc\left[(L+a)\sqrt{\frac{2mz}{\hbar^2}}\right] \tag{10.3}$$

10.2 Summation Formula for 3.21

To compute the sum in 3.21, we rely on formula 17.3.13 found on p. 243 of Hansen's *A Table of Series and Products* [16]:

$$\sum_{n=1}^{\infty} \frac{\cos\left[(2n-1)\,x\right]}{(2n-1)^2\,a^2-b^2} = \frac{\pi}{4ab}\sin\left[\left(\frac{\pi}{2}-x\right)\frac{b}{a}\right]\sec\left[\frac{\pi b}{2a}\right] \tag{10.4}$$

where $0 \le x \le \pi$. If $x_1 > x_2$, then we may assign Hansen's x to be $\dfrac{(x_1-x_2)\,\pi}{2a}$, his a to be our $\dfrac{\pi}{a}$, and his b to be our $\sqrt{\dfrac{8mz}{\hbar^2}}$. We can then write

$$\sum_{n=1}^{\infty} \frac{\cos\left[\frac{(2n-1)\pi}{2a}\,(x_1-x_2)\right]}{\frac{(2n-1)^2\pi^2}{a^2}-\frac{8mz}{\hbar^2}} = \frac{a}{4}\sqrt{\frac{\hbar^2}{8mz}}\sin\left[(a-x_1+x_2)\sqrt{\frac{2mz}{\hbar^2}}\right]\sec\left[a\sqrt{\frac{2mz}{\hbar^2}}\right] \tag{10.5}$$

and

$$\sum_{n=1}^{\infty} \frac{\cos\left[\frac{(2n-1)\pi}{2a}\,(x_1+x_2)\right]}{\frac{(2n-1)^2\pi^2}{a^2}-\frac{8mz}{\hbar^2}} = \frac{a}{4}\sqrt{\frac{\hbar^2}{8mz}}\sin\left[(a-x_1-x_2)\sqrt{\frac{2mz}{\hbar^2}}\right]\sec\left[a\sqrt{\frac{2mz}{\hbar^2}}\right] \tag{10.6}$$

10.3 Calculating $\langle x_1|\mathbf{G}_Q^o\mathbf{QHPG}_P^o\mathbf{PHQG}_Q^o|x_2\rangle$

As before, we begin with

$$\langle x_1|\mathbf{G}_Q^o\mathbf{QHPG}_P^o\mathbf{PHQG}_Q^o|x_2\rangle = \int_0^a\int_0^a dx_3dx_4\langle x_1|\mathbf{G}_Q^o|x_3\rangle\langle x_3|\mathbf{QHPG}_P^o\mathbf{PHQ}|x_4\rangle\langle x_4|\mathbf{G}_Q^o|x_2\rangle \tag{10.7}$$

and

$$\langle x_3|\mathbf{QHPG}_P^o\mathbf{PHQ}|x_4\rangle = \int_a^{L+a}\int_a^{L+a} dx_5 dx_6 \langle x_3|\mathbf{QHP}|x_5\rangle\langle x_5|\mathbf{G}_P^o|x_6\rangle\langle x_6|\mathbf{PHQ}|x_4\rangle \quad (10.8)$$

$$= \left(-\frac{2\hbar^2}{m}\right)^2 \int_a^{L+a}\int_a^{L+a} dx_5 dx_6 \partial x_5^{\rightarrow}\delta\left(x_5-a\right)\delta\left(x_3-x_5\right)\langle x_5|\mathbf{G}_P^o|x_6\rangle\partial x_6^{\leftarrow}\delta\left(x_6-a\right) \quad (10.9)$$

$$* \delta\left(x_4-x_6\right)$$

$$= \left(-\frac{2\hbar^2}{m}\right)^2 \int_a^{L+a}\int_a^{L+a} dx_5 dx_6 \delta\left(x_5-a\right)\delta\left(x_3-x_5\right)\partial x_5^{\rightarrow}\langle x_5|\mathbf{G}_P^o|x_6\rangle\partial x_6^{\leftarrow}\delta\left(x_6-a\right)$$

$$* \delta\left(x_4-x_6\right) \quad (10.10)$$

$$= \left(-\frac{2\hbar^2}{m}\right)^2 \int_a^{L+a}\int_a^{L+a} dx_5 dx_6 \delta\left(x_5-a\right)\delta\left(x_3-x_5\right)\partial x_5\partial x_6\langle x_5|\mathbf{G}_P^o|x_6\rangle\delta\left(x_6-a\right) \quad (10.11)$$

$$* \delta\left(x_4-x_6\right)$$

$$= \left(-\frac{2\hbar^2}{m}\right)^2 \int_a^{L+a}\int_a^{L+a} dx_5 dx_6 \delta\left(x_5-a\right)\delta\left(x_3-x_5\right) \quad (10.12)$$

$$* \partial x_5\partial x_6\left(-\sqrt{\frac{2m}{z\hbar^2}}\frac{\sin\left[\left(L+a-x_5\right)\sqrt{\frac{2mz}{\hbar^2}}\right]\sin\left[\left(x_6-a\right)\sqrt{\frac{2mz}{\hbar^2}}\right]}{\sin\left[L\sqrt{\frac{2mz}{\hbar^2}}\right]}\right)\delta\left(x_6-a\right)\delta\left(x_4-x_6\right) \quad (10.13)$$

$$= \left(-\frac{2\hbar^2}{m}\right)^2 \int_a^{L+a}\int_a^{L+a} dx_5 dx_6 \delta\left(x_5-a\right)\delta\left(x_3-x_5\right) \quad (10.14)$$

$$* \left(\sqrt{\frac{2m}{z\hbar^2}}\frac{2mz}{\hbar^2}\frac{\cos\left[\left(L+a-x_5\right)\sqrt{\frac{2mz}{\hbar^2}}\right]\cos\left[\left(x_6-a\right)\sqrt{\frac{2mz}{\hbar^2}}\right]}{\sin\left[L\sqrt{\frac{2mz}{\hbar^2}}\right]}\right)\delta\left(x_6-a\right)\delta\left(x_4-x_6\right) \quad (10.15)$$

$$= \frac{2\hbar^2}{m}\sqrt{\frac{2mz}{\hbar^2}}\cot\left[L\sqrt{\frac{2mz}{\hbar^2}}\right]\delta\left(x_3-a\right)\delta\left(x_4-a\right) \quad (10.16)$$

Note that integrating over a delta function that sits at the boundary of integration introduces

a factor of $\frac{1}{2}$. Returning to 10.7 (assume that $x_1 > x_3$ and $x_2 > x_4$),

$$\langle x_1|\mathbf{G}_Q^o\mathbf{QHPG}_P^o\mathbf{PHQG}_Q^o|x_2\rangle \tag{10.17}$$

$$= \frac{2\hbar^2}{m}\sqrt{\frac{2mz}{\hbar^2}}\int_0^a\int_0^a dx_3dx_4\langle x_1|\mathbf{G}_Q^o|x_3\rangle\cot\left[L\sqrt{\frac{2mz}{\hbar^2}}\right]\delta\left(x_3-a\right)\delta\left(x_4-a\right)\rangle\langle x_4|\mathbf{G}_Q^o|x_2\rangle \tag{10.18}$$

$$= \frac{\hbar^2}{2m}\sqrt{\frac{2mz}{\hbar^2}}\cot\left[L\sqrt{\frac{2mz}{\hbar}}\right]\langle x_1|\mathbf{G}_Q^o|a\rangle\langle a|\mathbf{G}_Q^o|x_2\rangle \tag{10.19}$$

$$= \frac{\hbar^2}{2m}\sqrt{\frac{2mz}{\hbar^2}}\cot\left[L\sqrt{\frac{2mz}{\hbar}}\right]\left(-\sqrt{\frac{2m}{z\hbar^2}}\sin\left[x_1\sqrt{\frac{2mz}{\hbar^2}}\right]\sec\left[a\sqrt{\frac{2mz}{\hbar^2}}\right]\right) \tag{10.20}$$

$$*\left(-\sqrt{\frac{2m}{z\hbar^2}}\sin\left[x_2\sqrt{\frac{2mz}{\hbar^2}}\right]\sec\left[a\sqrt{\frac{2mz}{\hbar^2}}\right]\right) \tag{10.21}$$

$$= \sqrt{\frac{2m}{z\hbar^2}}\sin\left[x_1\sqrt{\frac{2mz}{\hbar^2}}\right]\sin\left[x_2\sqrt{\frac{2mz}{\hbar^2}}\right]\sec\left[a\sqrt{\frac{2mz}{\hbar^2}}\right]^2\cot\left[L\sqrt{\frac{2mz}{\hbar^2}}\right] \tag{10.22}$$

Note that $x_1 < a$ and $x_2 < a$, and that this calculation does not depend on whether x_1 is less or greater than x_2.

10.4 Re-summing the S-matrix

We begin with equation 8.7

$$\mathbf{S} = \mathbf{U}_k^\dagger\frac{\mathbf{I}-i\mathbf{K}}{\mathbf{I}+i\mathbf{K}}\mathbf{U}_k^\dagger \tag{10.23}$$

$$= \mathbf{U}_k^\dagger\left(\mathbf{I}-\frac{2i\mathbf{K}}{\mathbf{I}+i\mathbf{K}}\right)\mathbf{U}_k^\dagger \tag{10.24}$$

Referencing equations 8.8 and 8.1 we can also define $\mathbf{K}$ by

$$\mathbf{K} = \boldsymbol{\omega}^T \frac{\mathbf{I}}{E\mathbf{I} - \mathbf{H}_{in}} \boldsymbol{\omega} \tag{10.25}$$

Hence,

$$\frac{\mathbf{K}}{I + i\mathbf{K}} = \left[\mathbf{I} + i\boldsymbol{\omega}^T \frac{\mathbf{I}}{E\mathbf{I} - \mathbf{H}_{in}} \boldsymbol{\omega} \right]^{-1} \boldsymbol{\omega}^T \frac{\mathbf{I}}{E\mathbf{I} - \mathbf{H}_{in}} \boldsymbol{\omega} \tag{10.26}$$

Using the geometric sum formula, we can write

$$\frac{\mathbf{K}}{I + i\mathbf{K}} = \sum_{n=0}^{\infty} (-i)^n \left(\boldsymbol{\omega}^T \frac{\mathbf{I}}{E\mathbf{I} - \mathbf{H}_{in}} \boldsymbol{\omega} \right)^n \boldsymbol{\omega}^T \frac{\mathbf{I}}{E\mathbf{I} - \mathbf{H}_{in}} \boldsymbol{\omega} \tag{10.27}$$

Which is equivalent to

$$\frac{\mathbf{K}}{I + i\mathbf{K}} = \boldsymbol{\omega}^T \sum_{n=o}^{\infty} (-i)^n \left(\frac{\mathbf{I}}{E\mathbf{I} - \mathbf{H}_{in}} \boldsymbol{\omega}\boldsymbol{\omega}^T \right)^n \frac{\mathbf{I}}{E\mathbf{I} - \mathbf{H}_{in}} \boldsymbol{\omega} \tag{10.28}$$

Employing the geometric series formula once more,

$$\frac{\mathbf{K}}{I + i\mathbf{K}} = \boldsymbol{\omega}^T \left(\mathbf{I} + i \frac{\mathbf{I}}{E\mathbf{I} - \mathbf{H}_{in}} \boldsymbol{\omega}\boldsymbol{\omega}^T \right)^{-1} \frac{\mathbf{I}}{E\mathbf{I} - \mathbf{H}_{in}} \boldsymbol{\omega} \tag{10.29}$$

$$= \boldsymbol{\omega}^T \frac{\mathbf{I}}{E\mathbf{I} - \mathbf{H}_{in} + i\boldsymbol{\omega}\boldsymbol{\omega}^T} \boldsymbol{\omega} \tag{10.30}$$

Substituting back into 10.24, we see that

$$\mathbf{S} = \mathbf{U}_k^\dagger \left(\mathbf{I} - 2i\boldsymbol{\omega}^T \frac{1}{E\mathbf{I} - \mathbf{H}_{in} + i\boldsymbol{\omega}\boldsymbol{\omega}^T} \boldsymbol{\omega} \right) \mathbf{U}_k^\dagger \tag{10.31}$$

Bibliography

[1] E. P. Wigner and L.E. Eisenbud, Phys. Rev. 72, 29 (1949)

[2] C. Bloch, Nucl. Phys. 4, 503 (1957).

[3] H. Feshbach, Ann. Phys. (N.Y.) 19, 287 (1962)

[4] Hoshik Lee and Linda E. Reichl, R-matrix theory with Dirichlet boundary conditions for integrable electron waveguides. Journal of Physics A: Mathematical and Theoretical, Vol. 43 (2010).

[5] Kyungsun Na and Linda E. Reichl, Electron Conductance and Lifetimes in a Ballistic Electron Waveguide. Journal of Statistical Physics, Vol. 92, Nos. 3/4 (1998)

[6] Gursoy B. Akguc and Linda E. Reichl, Conductance and Statistical Properties of Chaotic and Integrable Electron Waveguides. Journal of Statistical Physics, Vol. 98, Nos. 3/4 (2000)

[7] Gursoy B. Akguc and Linda E. Reichl, Effect of Evanescent Modes and Chaos on Deterministic Scattering in Electron Waveguides. Physical Review E, Vol. 64, 056221 (2001)

[8] Gursoy B. Akguc, Linda E. Reichl, Anil Shaji, and Michael G. Snyder, Bell States in a Resonant Quantum Waveguide Network. Physical Review A, Vol. 69, 0423XX (2004) 43.

[9] C. M. Marcus, A. J. Rimberg, R. M. Westervelt, P. F. Hopkins, and A. C. Gossard, Appl. Phys. Lett. Vol. 69, 506 (1992).

[10] M. A. Eriksson, R. G. Beck, M. Topinka, J. A. Katine, R. M. Westervelt, K. L. Campman, and A.C. Gossard, Appl. Phys. Lett. Vol. 69, 671 (1996).

[11] J. P. Bird, R. Akis, D. K. Ferry, A. P. S. de Moura, Y.-C. Lai, and K. M. Indlekofer, Rep. Prog. Phys. Vol. 66, 1 (2003).

[12] S. Datta, Electronic Transport in Mesoscopic Systems. Cambridge University Press, Cambridge, 1995.

[13] Agapi Emmanouilidou and Linda E. Reichl, Scattering Properties of an Open Quantum System. Physical Review A, Vol. 62, 022709 (2000)

[14] Linda E. Reichl, The Transition to Chaos: Conservative Classical Systems and Quantum Manifestations. Springer, 2004. p. 297-310, 330-335.

[15] Norman W. McLachlan, Complex Variable Theory and Transform Calculus with Technical Applications. Cambridge University Press, Cambridge, 1953. p. 54

[16] Eldon R. Hansen, A Table of Series and Products. Prentice Hall, May 1975. p. 243

Vita

William Zachary Corse was born in Bethesda, Maryland on 28 February 1989, the son of Dr. William R. Corse and Donna M. Corse. He received a Bachelor of Science degree in Physics from Duke University in May, 2011. He started graduate studies in physics at the University of Texas at Austin in August, 2012.

Permanent address: 105 Wynfield Lane
New Hope, PA 18938

This thesis was typeset with LaTeX[†] by the author.

[†]LaTeX is a document preparation system developed by Leslie Lamport as a special version of Donald Knuth's TeX Program.